UNIVERSITÀ DI SIENA 1240

Dipartimento di **Biotecnologie Mediche**

Dottorato in "Genetics, Oncology and Clinical Medicine" (GenOMeC)

35° Ciclo (2019-2022)

Coordinatrice: **Prof.ssa Francesca Ariani**

The profibrogenic role of neutrophil extracellular traps in stenotic Crohn's disease: a new antifibrotic target

Settore scientifico disciplinare: **MED/12**

Candidato

Dr. Gabriele Dragoni

Dipartimento di Scienze Biomediche, Sperimentali e Cliniche "Mario Serio", Università di Firenze (IT)

Firma digitale del candidato

GABRIELE DRAGONI 07.03.2023 17:39:17 GMT+01:00

Supervisore

Prof. Andrea Galli

Dipartimento di Scienze Biomediche, Sperimentali e Cliniche "Mario Serio", Università di Firenze (IT)

Co-supervisore

Prof. Alessandro Maria Vannucchi

Dipartimento di Medicina Sperimentale e Clinica, Università di Firenze (IT)

Anno accademico di conseguimento del titolo di Dottore di ricerca

2021/22

Università degli Studi di Siena
Dottorato in "Genetics, Oncology and Clinical Medicine" (GenOMeC)
35° Ciclo

Data dell'esame finale
21 marzo 2023

Commissione giudicatrice

Prof. Andrea Galli
Dip. Di Scienze Biomediche, Sperimentali e Cliniche "Mario Serio", Università di Firenze

Prof. Flavio Caprioli
Dipartimento di Fisiopatologia Medico-Chirurgica e dei Trapianti dell'Università degli Studi di Milano

Prof.ssa Giulia Martina Cavestro
Unità di Gastroenterologia ed Endoscopia Digestiva dell'IRCCS Ospedale San Raffaele

Supplenti

Prof.ssa Francesca Ariani, Dipartimento Di Biotecnologie Mediche, Università di Siena

Prof. Francesca Pentimalli, Dipartimento di Medicina e Chirurgia - Università LUM Giuseppe Degennaro Casamassima (BA)

INDEX

ABSTRACT

BACKGROUND: Neutrophil extracellular traps (NETs) are structures of DNA filaments and protein granules, extruded by neutrophils after insults in a PAD4-dependent manner. In autoimmune events, their release occurs early during inflammation, further aggravating tissue injury and presumably contributing to fibrosis. Our aim was to investigate the potential profibrotic effect of NETs in stenotic Crohn's disease (CD).

METHODS: Immunofluorescence (IF) for PAD4, NETs markers and fibroblast activation protein (FAP) was performed on resected ileum derived from patients with stricturing CD. Human intestinal fibroblasts (HIF) were extracted from unaffected CD ileum. A CCD-18Co fibroblast line was used as confirmation. In vitro co-cultures of subconfluent HIF with NETs were performed for 24 hours, and RNA extracted for sequencing. Soluble collagen released in culture medium was quantified with SIRCOL®. Migratory activity was investigated with scratch test. IF intensity of collagen and FAP was quantified using Operetta®. Transfection of CCD-18co cells with NF-kB-luciferase reported plasmid was performed to evaluate the TLR2/NF-kB pathway. Specific inhibitors (C29 and CAPE) were used to block TLR2 and NF-kB activity, respectively. Finally, a chronic DSS mice model of intestinal fibrosis with selective PAD4 knock-out in neutrophils ($PAD4^{fl/fl}MRP8^{Cre+}$) was used as confirmation. Picrosirius red staining and SIRCOL® were used to quantify the collagen amount after sacrifice.

RESULTS: IF on inflamed ileum showed clusters of NETs close to FAP^+ fibroblasts, suggesting in vivo interactions. Transcriptomics demonstrated an upregulation of profibrotic genes and toll-like pathways ($p<0.05$) in the group of HIF stimulated with NETs. Increased proliferation rate, slower wound healing ability and higher collagen release in the medium were observed in NETs group, as well as higher IF expression of collagens and FAP. Transfection showed significant upregulation ($p=0.015$) of NF-kB in NETs group, whereas its expression and soluble collagen release decreased using C29 and CAPE. Accordingly, phospho-NF-kB and MyD88 proteins were increased in NETs group. A significantly lower amount of collagen was measured in the colon of PAD4-knocked out mice both with Picrosirius red ($p=0.04$) and SIRCOL® ($p=0.008$), as well as reduced FAP^+ fibroblasts at IF.

CONCLUSION: NETs may represent an early trigger of fibroblast activation in the intestine via the TLR2/NF-kB axis. As NETs are also early players during inflammation, blocking PAD4 might improve both inflammation and fibrogenesis in CD.

INTRODUCTION

1. Crohn's disease and intestinal fibrosis

Crohn's disease (CD) is a chronic inflammatory condition that can involve any part of the bowel from mouth to anus in a discontinuous manner, with terminal ileum and right colon as the most frequently affected segments[1]. Its pathogenesis is currently unclear and complex, with environmental triggers and gut microbiota that have been shown to shape the immune response towards the intestinal tissue in individuals with genetic predisposition[2]. The chronic intermittent damage to the intestinal layers may result in excessive repair, i.e., intestinal fibrosis, thus leading to a stricturing phenotype in more than half of the patients[3,4]. The final outcome may be bowel obstruction with the need of hospitalization and interventions, such as endoscopic dilation or the more frequent intestinal resection.

Currently, no biomarker has been validated for the follow-up of patients with inflammatory and stenotic CD to monitor disease activity, facilitate clinical trial endpoints and anticipate potential complications in high-risk patients[5]. Moreover, although several agents have shown promising results in preclinical studies, no antifibrotic therapy has shown satisfying results in controlling and/or reversing the fibrotic process. Therefore, a whole and comprehensive understanding of the pathophysiological mechanisms at the basis of intestinal fibrosis is necessary to tackle this issue and have an impact on clinical practice of CD.

2. Intestinal fibrosis

Fibrosis is the result of excessive production of extracellular matrix (ECM) by activated mesenchymal cells. In the spectrum of wound healing, defined as the physiological process through which a tissue responds to injury with the aim of repair, fibrosis represents the opposite pole. In fact, it is defined as a dysregulated and uncontrolled repair activity.

In the intestine, this process is triggered by external damage and mucosal insults that activate the inflammatory cascades. As inflammation is associated with ulcers and so with loss of superficial mucosa, it is intuitive to believe that fibrogenesis "starts" in the

submucosal layer. Once activated, this pathological process is self-perpetuating, independent from inflammation[6-9]. The replacement of normal tissue with ECM deposition results in loss of function, such as malabsorption, loss of motility and gut lumen reduction.

Basic research of intestinal fibrosis presents many issues. First, we do not have a validated histological score to define different levels of fibrosis, thus limiting objective measurements during lab experiments. Moreover, the only exhaustive information on human samples come from surgical resections, that allow transmural assessment of the bowel wall. Otherwise, it is difficult to study intestinal fibrosis in human because endoscopic biopsies are too superficial (sampling mucosa and rarely the most superficial layer of submucosa) and stenotic/narrow areas are often not accessible with the endoscope. To further complicate its study, many cellular and molecular components actively participate to fibrogenesis, and these will be extensively discussed in the next paragraphs.

2.1 Histopathology

Histopathological analysis from surgical resections is the gold standard to accurately define the presence of intestinal fibrosis within a stricture. Currently, no validated histology score is available. Recently, an international consensus proposed the key histological findings that must be present on hematoxylin & eosin examination in order to score properly small bowel stricturing disease[10]. A fundamental aspect to diagnose a small bowel stricture is the evidence of fibrosis of the submucosa, and this should be defined as "an increased collagen content in the stricture section compared with any other non-stricture section"[10]. In addition, other items may sit aside, such as increased thickness of all wall layers and muscularization of the submucosa (or increased thickness of the muscolaris mucosa), that implies a hyperproliferation of mesenchymal cells. Fibrotic septa between submucosal and muscle layers are often present in advanced cases, as well as subserosal fibrosis[11] (**Figure 1**).

A more objective evaluation of fibrosis can also be performed by quantifying the amount of collagen in a transmural section. This can be done with the use of specific stainings that bind to collagen, such as Masson's trichrome and Picrosirius red. In detail, Masson's

trichrome is the most popular and the most broadly performed for the study of fibrosis. It uses three different dye solutions that bind to specific proteins, resulting in the following stainings: keratin and muscle in red, collagen and bone in blue, and cytoplasm in light red. On the other hand, Picrosirius red is a dye with particular optical properties that has shown high precision in the study of collagen content. Although binding to many different proteins, it orients parallel to collagen fibrils only, greatly enhancing their natural birefringence. As such, the complexes made of Picrosirius and collagens are much more birefringent than those formed with other proteins, and so stand out against the dark background under polarized light[12].

In general, the composition of the ECM can be used as an indicator of either physiological or dysregulated tissue repair. Collagen I and III have been linked to regular wound healing, whereas Collage IV and VI are more associated with excessive fibrosis[13]. In a specific study on CD, consistent results have been reported[14].

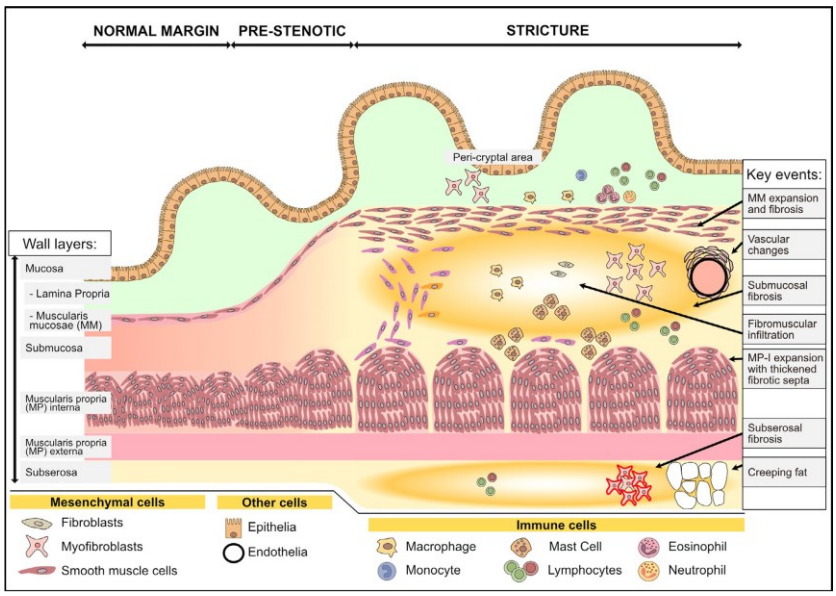

Figure 1: Representation of wall layers and key events occurring in the development of intestinal fibrosis in a stenotic intestine. Image from: Alfredsson J et al. Scand J Immunol. 2020.[11]

2.2 Cellular components

Many cellular types participate to the process of intestinal fibrosis. Briefly, these cell lines may be divided in two different groups: the activated myofibroblasts (aMF) and the supporting compartments. The aMF are cells with migratory and contractile activity, producing collagen and other ECM components, representing the principal players of

fibrogenesis[15]. In the past, they were thought to be identified by the marker alpha-smooth muscle actin (αSMA), but we now know that their characteristic marker of activation in the intestine is the fibroblast activation protein (FAP), which is positively expressed in the majority of aMF in strictures[16,17]. Moreover, the inhibition of FAP has been shown to result in reduced collagen secretion and increased migration of aMF[17]. Whilst in other organs aMF are derived from few cellular populations, in the intestine they may differentiate from two groups of cells, namely resident mesenchymal cells (intestinal fibroblasts, quiescent myofibroblasts and muscle cells[18]) and additional cells. Among the latter group, it is worth mentioning the mesenchymal transition of epithelial and endothelial cells (epithelial-to-mesenchymal transition and endothelial-to-mesenchymal transition, respectively), but also pericytes, stellate cells and bone marrow derived fibrocytes (**Figure 2**).

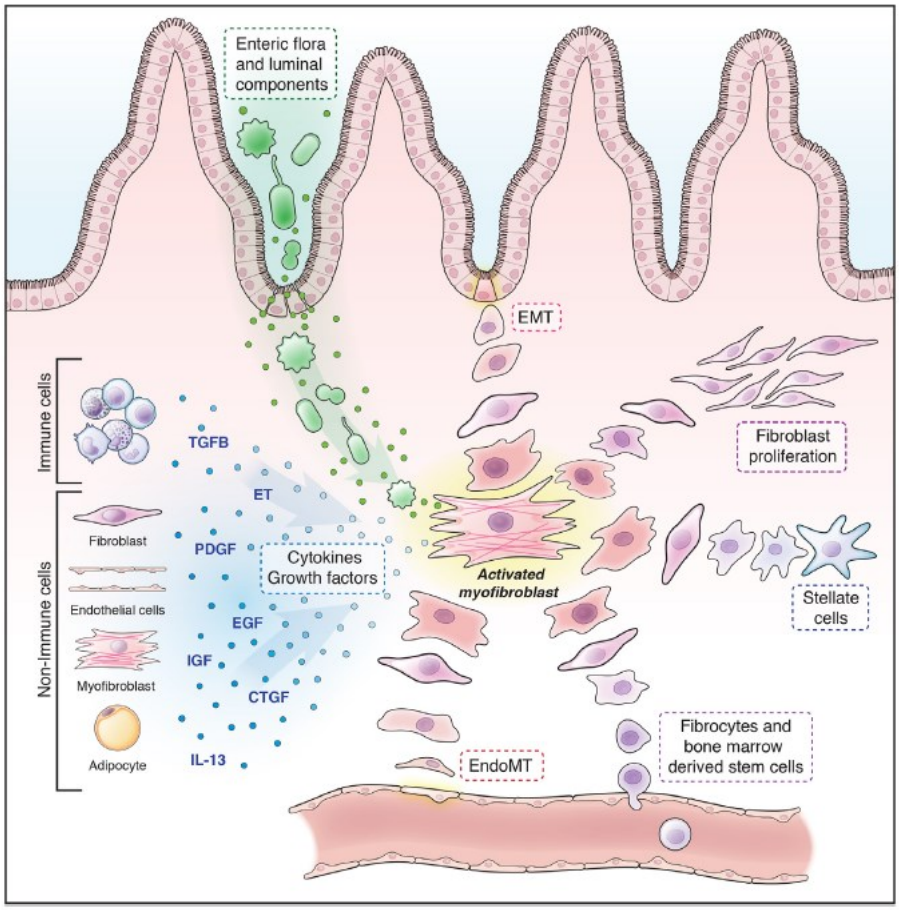

Figure 2: Cellular players contributing to the pool of activated myofibroblasts in the context of intestinal fibrosis. Image from: D'Haens G et al. Gastroenterology 2022.[15]

Cells supporting aMF function of which we have the most convincing evidence are mainly monocytes/macrophages and lymphocytes. Macrophages are well known for their plasticity that allow them to respond differently depending on the extracellular milieu[19] (**Figure 3a**). Therefore, in the initial phases of tissue damage, they are more prone to have a pro-inflammatory phenotype with an apoptotic effect on myofibroblasts. The subsequent step is what determines the tissue healing towards either resolution of inflammation and fibroblast inactivation (with regulatory macrophages) or tissue fibrosis and stimulation of aMF (with profibrotic macrophages). Regarding lymphocytes, Th1 population is an antifibrotic regulator with its interfering action due to interferon(IFN)-gamma production[20]. On the other hand, Th2 lymphocytes present a profibrotic activity, mainly due to the release of IL-13[20]. Lately, a third subgroup of lymphocytes has shown an important profibrotic role, the Th17. In fact, the most important cytokine released by the Th17, i.e., IL-17a, has demonstrated to stimulate aMF to upregulate ECM deposition and remodelling[21] (**Figure 3b**).

However, although the immune response in the mucosal layer is well characterized, little is known about the mechanisms involving the immune cells in deeper layers of strictures as well as cell-cell interactions[11].

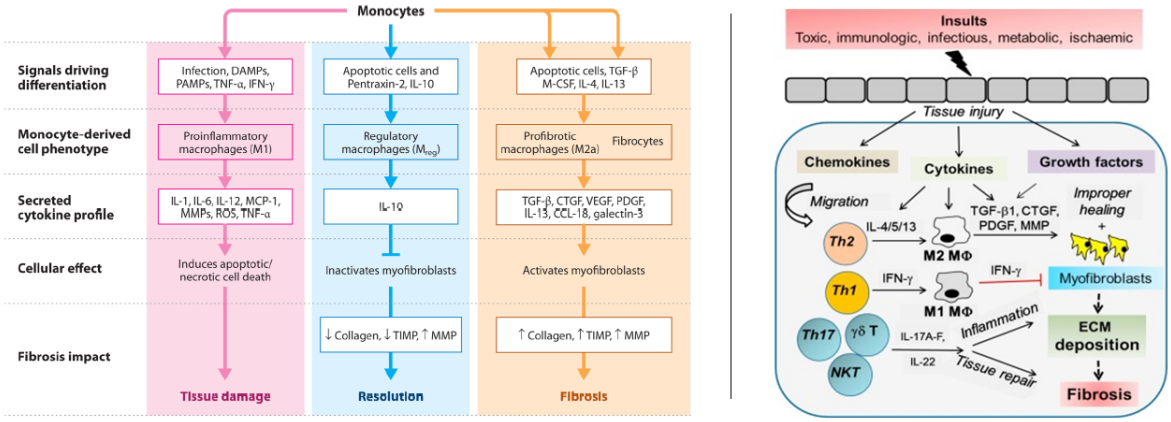

a. b.

Figure 3: Mechanisms by which monocytes and lymphocytes modulate and control fibroblast activity. Images are taken from Duffield JS et al. Annu Rev Pathol. 2013[19] (**a.**) and from Ramani K et al. Cytokine. 2019[21] (**b.**).

2.3 Molecular components

From a molecular point of view, the main drivers of myofibroblast activation and transition are numerous and complex, with many cytokines, growth factors and also microbiota components among them. In physiological conditions, production and degradation of ECM are under the control of metalloproteinases (MMPs) and tissue inhibitors of metalloproteinases (TIMPs). Whenever a dysregulation of MMP/TIMP balance exists in the gut, ECM accumulation and thus intestinal fibrosis occur[20]. Particularly in CD, the equilibrium of MMP/TIMP is disturbed, more vigorously in case of active disease and intestinal strictures[22,23].

Among the different involved mechanisms, transforming growth factor-beta (TGFβ) signalling through the TGFβ/SMAD pathway certainly represents the "core" pathway[24] (also known as "canonical" pathway, **Figure 4a**). Particularly with its isoform 1, TGFβ regulates and amplifies the fibrotic process both in the intestine and in many other extraintestinal tissues. It is mainly produced by monocytes/macrophages, but a lower amount is also released by the same fibroblasts in autocrine manner. Downstream activation of SMAD2/3 and connective tissue growth factor (CTGF) determines an increase in proliferation and survival of fibroblasts, an upregulation of collagen production and a promotion of mesenchymal transition of epithelial and endothelial cells[7,25] (**Figure 4b**). Moreover, TGFβ reduces MMPs activity and ECM digestion together with reducing fibroblasts migration. Unfortunately, blocking TGFβ has not provided the expected results in terms of reducing fibrosis, since this cytokine controls many immune functions, including regulatory T-cells activity, resulting in worsening the inflammatory insult and ultimately the fibrotic process. However, this pathway remains crucial as main reference to study the effect of other profibrogenic molecular mechanisms.

Since the intestine is a non-sterile environment, fibrogenesis may also be influenced by gut microbiota, with evidence that is starting to accumulate[26]. For example, a pre-treatment with an antibiotic cocktail in a mouse model of radiation enteritis has demonstrated to reduce the TLR4/MyD88/NF-kB pathway and thus also the level of intestinal fibrosis linked to this[27]. Similarly, it has been shown that murine models without microflora do not develop intestinal fibrosis[28]. However, the modulation of the microbial

environment is a delicate matter and many more data are needed for a fully comprehensive understanding.

Moreover, the same ECM composed of structural (collagen and elastin) and functional (e.g., fibronectin) proteins has been shown to play an active role in fibrogenesis rather than represent a passive scaffold that replaces the damaged tissue. In fact, TGFβ is present in a latent form into the matrix and shear stress forces of the aMF may facilitate its release, thus stimulating a positive feedback of profibrogenic mechanisms in mesenchymal cells[29]. In addition, matrix networks within the ECM lead to increased stiffness of the tissue, that can consequently activate aMF with a positive feedback, even without inflammation[30].

Independently from the causal agent, damage to the intestinal mucosa triggers an acute inflammatory response that sees cells of the innate immunity (monocytes/macrophages, neutrophils etcetera) as the first actors. It has already been discussed the role of macrophages in the fibrotic process, but also cytokines and chemokines included in neutrophil granules have shown profibrotic properties[20]. Therefore, blocking the harmful and fibrogenic activity of neutrophils may avoid potential downstream cascades, since neutrophils are among the first cells to react to mucosal damage. This idea is what guided the entire research of this PhD thesis, which will be discussed more thoroughly in the next introductive paragraphs.

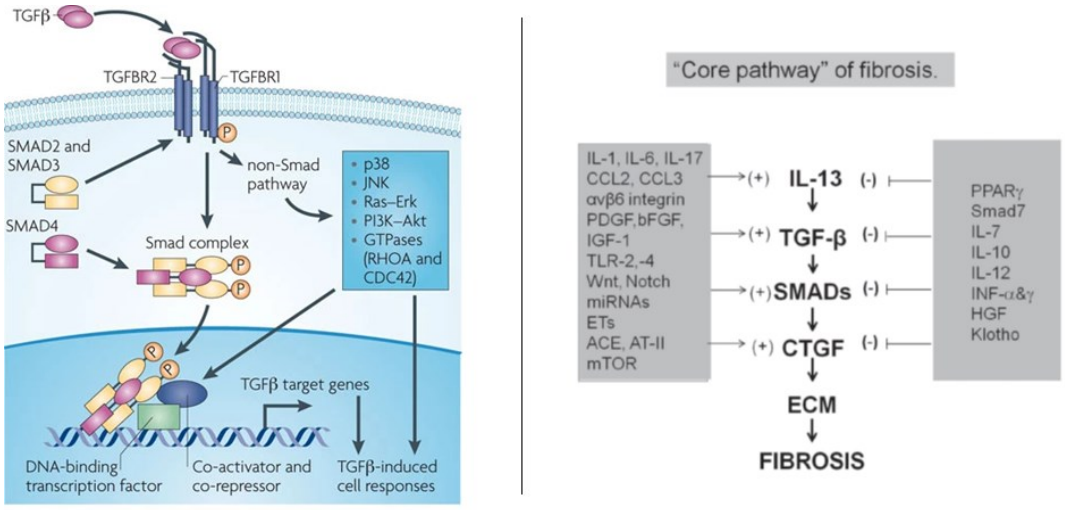

a. b.

Figure 4: Representation of the downstream consequences of TGFβ/SMAD pathway activation. Images are taken from Ikushima H et al. Nat Rev Cancer. 2010[31] (**a.**) and from Latella G et al. JCC. 2014[25] (**b.**).

2.4 Animal models

In vivo confirmations of bench experiments are necessary to comprehend whether the pathogenic mechanisms have a strong impact in the process under investigation. With regard to intestinal fibrosis, many animal models have been developed although none can truly recapitulate the chronic and complicated nature of inflammatory bowel disease (IBD)[25]. These models can be divided into 7 categories:

1) spontaneous: the SAMP1/Yit is the most representative since disease occurs spontaneously with segmental and transmural lesions in the ileum together with granuloma that are very similar to CD[32].

2) chemically induced: this group is represented by the trinitrobenzenesulphonic acid (TNBS) and dextran sodium sulphate (DSS) chronic models of fibrosis[33,34]. This type of model is currently the most broadly used for its simplicity, reproducibility and low costs. Briefly, chemical insult is responsible of tissue damage through the course of multiple cycles, simulating the chronic, intermittent nature of IBD.

3) bacteria-induced: in this case an infectious agent is used. Among them, we may find the S. typhimurium[35], the adherent-invasive E. Coli[36], and the peptydoglican-polysaccharide[37].

4) immune-mediated: this has been more extensively used to study the immune-mediated events rather than fibrosis *per se*. An example is the injection of T-cells CD4+ $CD45RB^{high}$,[38] and since T cells are intimately linked to fibrosis in IBD, the investigation of fibrotic processes in this model could be of use.

5) radiation induced: the use of radiation causes inflammation and fibrosis similar to that of CD, with myofibroblasts and muscle cells proliferation, vascular sclerosis and the formation of chronic ulcers[39].

6) post-operative: this model consists in performing an ileo-caecal resection in IL-10 knock-out mice and observe the development of subsequent fibrosis in the small intestine[40]. This model is certainly useful in case the main aim is to study the occurrence of fibrosis proximal to the anastomosis.

7) gene knockout and transgenic: this model is definitely more expensive than the others, examples are the IL-10[40,41] or the TGFβ/Smad[42] knock-out models.

8) mechanic injury: a recent protocol has demonstrated that it is possible to develop transmural intestinal fibrosis by repeating intestinal biopsies during endoscopy[43]. The major drawback of this model is the learning curve for the researchers as well as the fact that it determines colon strictures whereas most of the stenoses occur in the small bowel.

Current animal models of intestinal fibrosis present an important limitation: a preceding stage of chronic inflammation almost necessarily needs to occur to start the fibrotic process. This overlap is associated with an overwhelming barrier as it makes almost impossible to dissect independent immunological pathways that control inflammation and fibrosis[44].

Although very promising for the future, the use of intestinal organoids in the context of fibrogenesis has only started to propose experimental models to be adopted for studies in the field[45].

3. Neutrophil extracellular traps (NETs)

3.1 General aspects

Neutrophils are cells of the innate immunity that are among the first to intervene during inflammatory insults. *Neutrophil extracellular traps* (NETs) are "web-like" structures made of DNA filaments and protein granules released by neutrophils during different stimuli, such as response against pathogens, thromboembolic events, autoimmunity, atherosclerosis, cancer, etcetera[46]. Citrullination of histones H1 and H3 by the enzyme peptidyl arginin deiminase 4 (PAD4) is the fundamental process to decondense the chromatin in the nucleus of neutrophils, facilitating the expulsion of chromosomal DNA[47]. This occurs in the event of NADPH-dependent production of reactive oxygen species (ROS), that increase calcium influx and subsequent PAD4 activation[48]. The phenomenon is nowadays called "*suicidal NETosis*", in contrast with "*vital NETosis*" (**Figure 5**). The latter has been more recently described as a similar process, but independent of oxidants, in which the plasma membrane is not disrupted and NETs are extruded by vesicles and blebbing, preserving the integrity of neutrophils[49]. From their discovery less than 20 years ago[50], it is not yet clear what their precise role is during inflammation and which downstream pathways they can activate in addition to pathogen

killing. Since "*vital NETosis*" has been correlated more with response to pathogens than sterile inflammation[51], we will mainly refer to "*suicidal NETosis*" throughout this work.

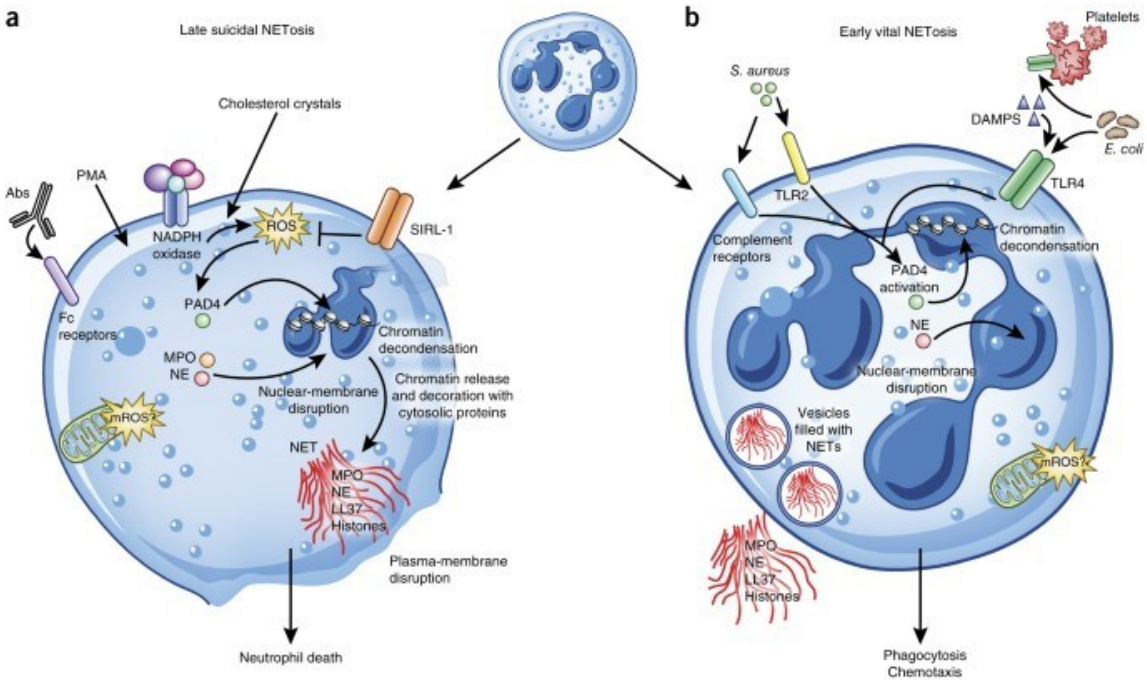

Figure 5: Schematic overview of "*suicidal*" and "*vital*" NETosis. Picture from Jorch SK et al. Nat Med. 2017[49].

3.2 NETs and IBD

In the field of IBD, data are starting to accumulate with regard to the role of NETs during the inflammatory insult[52]. The presence of inflammatory and oxidative triggers in the gut of IBD patients represents the perfect environment to stimulate NETs formation, with cytokines (IL-6, TNFα, IL1β), microbial products and DAMPs (damage associated molecular patterns) as main activators[53] (**Figure 6**). In the first study on the matter, proteomic analysis of colic biopsies showed that the expression of neutrophils and NETs correlated with histologically inflamed mucosa in patients with ulcerative colitis (UC) that were in endoscopic remission[54]. Additional evidence on histology analysis from ileo-colonic biopsies and metaproteomics of faecal samples of CD patients and colonic biopsies from UC patients confirmed the abundant presence of NETs in both active IBD compared to healthy controls and inactive IBD cases[55-57]. On the other hand, conflicting evidence from two other studies have shown the exclusive occurrence of NET formation in UC but not in CD[58,59], probably due to small cohorts and heterogeneous sampling of

ileal and colonic biopsies. However, the abundance of NETs has been directly correlated with the severity of inflammation described at histology in endoscopic biopsies of patients with CD[60]. In addition, the use of Cl-amidine and striptonigrin, a generic PAD inhibitor and a selective PAD4 inhibitor respectively, has demonstrated to reduce the inflammatory burden in a mouse DSS model of acute colitis[58,61]. Other authors have also claimed a similar effect by using an inhibitor of myeloperoxidase (MPO)[62]. Very recently, NETs localisation has also been reported in perianal fistulas of CD patients, with particular abundance in the ones with unhealed post-operative fistulas[63].

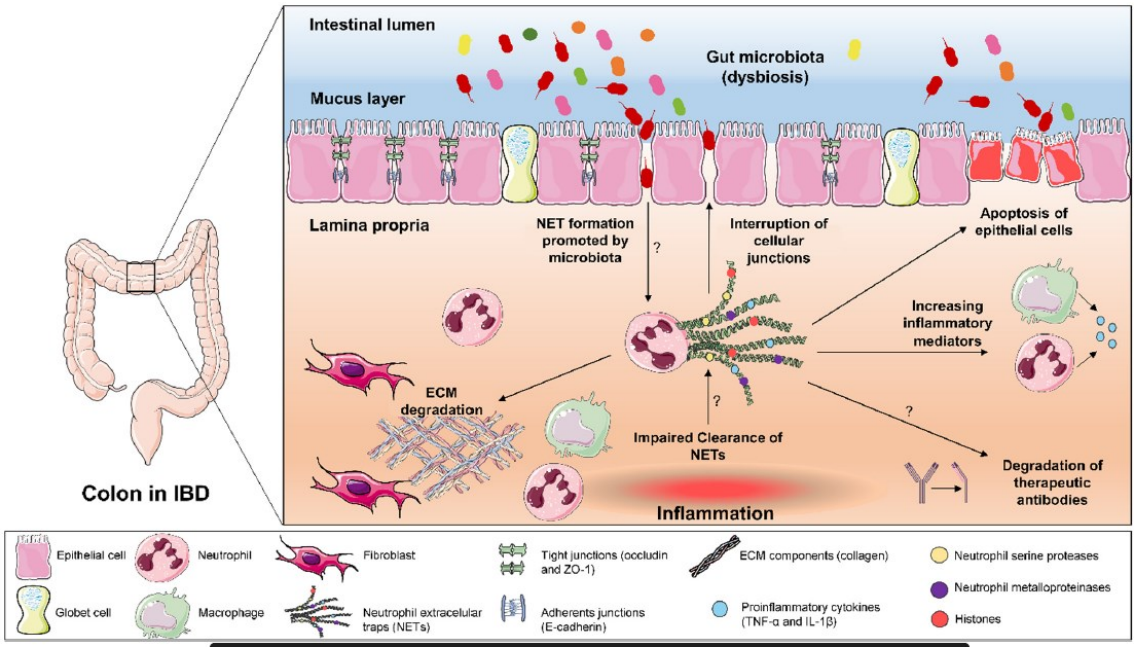

Figure 6: Proposed role for NETs in the gut. Their multiple functions may explain and perpetuate chronic inflammation and the occurrence of fibrosis. Picture from Dos Santos Ramos A et al. Pharmacol Res 2021[53].

NETs have also been linked to the activation of a hypercoagulable state: their presence was reported in the peripheral blood of patients with active IBD, but not in the ones in remission[64]; similarly, neutrophils from active IBD patients showed more spontaneous NET formation than inactive patients and healthy individuals, together with increased thrombotic tendency[65]. Moreover, the use of DNase to digest the DNA filaments of NETs has shown to significantly decrease platelet activation and the formation of thrombi in a mouse model of DSS colitis, as well as to attenuate the colitis burden[56]. On the other hand, the concept of harmful NETs has been recently challenged by the group of Markus

Neurath, that reported a beneficial role of immunothrombosis[66]. In their acute DSS model of colitis, PAD4-/- mice suffered from a more severe course of colitis than controls with significant increase in rectal bleeding due to impaired blood clot remodelling, thus leading to incomplete and delayed wound healing[66]. Therefore, the authors concluded that IBD treatment should carefully focus on balancing neutrophil response rather than eliminate it, as neutropenia has shown in general to induce neutropenic enterocolitis[67].

More in general, patients with IBD are more prone to form NETs as suggested by two works in which serum from IBD patients and medium from *ex vivo* cultures of inflamed mucosa enhanced NETs formation[59,64]. Thus, a better understanding of the consequences of this phenomenon is crucial to tackle the pathogenesis of IBD both in inflammation and fibrosis fields.

3.3 NETs and fibrosis

In the previous paragraphs, it has been mentioned that fibrosis is triggered by inflammation and then can perpetuate independently. Finding the upstream players of this trigger may potentially block fibrogenesis from the very beginning. In this context, as neutrophils are the first cells of the innate immunity that respond to damage, it might be interesting to study the role of NETs and their interactions with activated fibroblasts. In a physiological wound healing, neutrophil response is limited to the acute wound setting. However, neutrophils have been demonstrated to play an active role in chronic wounds for an extended period[68].

The first pivotal study demonstrating a potential profibrotic effect of NETs on fibroblasts is the one of Chrysanthopoulou and colleagues[69]. In their *in vitro* experiments, they showed that co-culturing primary lung fibroblasts with NETs derived from healthy volunteers can result in activation of fibroblasts into aMF with subsequent enhanced connective tissue growth factor (CTGF) and collagen production, and increased proliferation/migration rate[69]. In the same study, a co-localisation of aMF and NETs was seen both in interstitial lung disease and in skin scar tissue at immunofluorescence, suggesting common processes in different organ environments. These data on lung fibroblasts were later confirmed by a study on polymyositis-related interstitial lung disease, where NETs promoted fibroblast activation through TLR9/miR-7/Smad2

pathway[70]. Another indirect evidence of this potential interaction was provided by a mouse model of age-related fibrosis, where a reduced level of fibrosis was reported in the heart and in the lung of PAD4-knockout mice compared to the wild-type group, due to a reduced formation of NETs[71]. Recently, in a mouse model of laminectomy, it has been shown that NETs are able to boost the scar formation in post-epidural fibrosis by facilitating the expression of fibronectin macrophages, and this was significantly reduced with DNase-I, which digested DNA trap filaments[72]. Accordingly, PAD4-knockout mice undergoing bleomycin-induced lung fibrosis presented less NETs abundance and reduced mRNA levels of collagen 1A1, elastin, fibronectin and CTGF, resulting in ameliorated pulmonary fibrosis when compared to controls[73]. Similarly, in a murine model of osseointegration failure, PAD4-knockout mice (or the use of DNase-I) showed reduced fibrotic tissue repair and improved osseointegration, suggesting a perpetuating inflammatory effect of NETs as the cause of impaired healing[74]. In an elegant study on chronic thrombosis, it has been recently shown that NETs promote fibrotic thrombus remodelling via upregulation of TGFβ pathway in fibroblasts, which were also showing increased levels of αSMA and FAP when stimulated with NETs[75]. Moreover, the in vitro co-culture of MLE-12 cells (murine lung epithelial cells) with NETs was found to determine significant profibrotic characteristics and EMT, associated with increased levels of TGFβ1 in the medium[76].

It has been recently speculated that NETs may activate fibroblasts through different mechanisms linked to the released of certain proteins. For example, LL-37 can bind to a G-coupling receptor on fibroblasts (FPRL1) resulting in increased production of collagen; moreover, internalisation of neutrophil elastase may favour the trans-differentiation of fibroblasts into aMF with enhanced contractility[77]. In addition, interleukin (IL)-17A released with NETs could also have a profibrogenic boost on fibroblasts[78]. Many of these hypotheses have not yet been clearly proved with further publications. On the other hand, a high concentration of elastase has been shown to favour ECM degradation and delay regular healing[79], probably inducing an indirect hyperactivation of aMF. In accordance, in a mouse model of excisional skin wounds, PAD4 knock-out mice presented accelerated wound healing, suggesting that NETs may impair initial healing process, such as re-epithelialization[80], and this was later confirmed in diabetic foot ulcer patients[81], primary and secondary wound healing[82], and in a mouse model of wound-induced hair follicle neogenesis[83].

To date, no studies have been performed regarding this phenomenon in the gut. In an elegant work that combined bulk and single-cell transcriptomics with histopathology and *in situ* localization, it has been demonstrated that activated FAP^+ fibroblasts present neutrophil-chemoattractant properties in the ulcer bed, thus suggesting interactions between these two populations during chronic inflammation[84]. However, the key role of NETs in wound healing remains poorly understood and inadequately studied[85].

4. Toll-like receptor (TLR) signalling and fibrosis

Toll-like receptors (TLRs) are receptor involved in recognition of molecules, such as DAMPs and PAMPs. Ten different isoforms belong to the family, from TLR1 to TLR10. Among them, TLR1, TLR2, TLR4, TLR5 and TLR6 are present on the cell surface, the others are in intracellular vescicles[86]. Growing evidence is linking the activation of TLR cascades not only to inflammation but also to tissue fibrosis. For example, TLRs are involved in the induction of peritoneal EMT[87], and TLR2 has been shown to regulate heart remodelling by shaping the production of collagen I and III and reducing high-fat-induced cardiac fibrosis[88-90]. Similarly, TLR2/MyD88/NFkB pathway has been demonstrated to be crucial in bleomycin-induced pulmonary fibrosis[91]. In the liver, $TLR^{-/-}$ mice had reduced hepatic fibrogenesis than wild-type when exposed to CCl_4 treatment[92], and this was also confirmed by more selective TLR5 deficiency[93]. In all these studies, a global evaluation of TLRs has been considered, without focussing on the expressing cell and pathogenic mechanism that is associated to fibrosis (probably as a consequence of inflammation). Nonetheless, selective deletion of MyD88 (intracellular downstream signal of TLRs) in αSMA^+ intestinal fibroblasts has been demonstrated to reduce the degree of intestinal fibrosis in mice, showing a direct link between TLR response and intestinal fibrogenesis[94].

During *NETosis*, DNA filaments and associated nuclear proteins, such as histones, may act as DAMPs and exert direct activation of TLR in effector cell lines. Some studies have already shown that NETs are able to communicate with other cells by activating the TLR signalling. For example, NETs promote Th17 cell activation and differentiation through TLR2 downstream cascade[95]. NETs also convert platelets and endothelial cells to a procoagulant phenotype partially through TLR2 and TLR4[56]. In addition, NETs have shown to promote *in vitro* lung fibroblast activation and differentiation in aMF through

TLR9/miR-7/Smad2 signalling[70]. Therefore, intestinal fibroblasts may potentially be activated by NETs in the same manner.

AIM OF THE STUDY

The aim of this project was to study a potential link between the early occurrence of neutrophil response during inflammation and the subsequent activation of profibrotic phenotype in intestinal fibroblasts. Particularly, we aimed to investigate whether NETs are able to trigger the fibrotic process by enhancing collagen production in fibroblasts of patients with CD.

Part of the experiments was carried out at the “Inflammatory Bowel Disease Unit” and the “Laboratory of Mucosal Immunology” of TARGID (Transalational Research Center for Gastrointestinal Disorders), Katholieke Universiteit Leuven (Leuven, Belgium) under the supervision of Prof. Dr. Séverine Vermeire and Prof. Gianluca Matteoli. The remainder was performed at the local “Gastroenterology Research laboratory” of the Department of Experimental and Clinical Biomedical Sciences “Mario Serio”, University of Florence (Florence, Italy) under the supervision of Prof. Andrea Galli.

MATERIALS AND METHODS

1. Patient inclusions

Patients with Crohn's disease (CD) undergoing ileal or ileocolic resection for fibrostenotic complication were recruited between March 2019 and February 2020 at the University Hospital of Leuven (Belgium). Exclusion criteria were: presence of enteric fistula with or without abscesses, isolated colonic disease, age <18 years, ongoing immunosuppressive treatment without appropriate washout, active cancer. For each CD specimen, three different macroscopic areas were identified and histologically confirmed by an expert pathologist, i.e., proximal unaffected ileum, inflamed ileum, and fibrotic ileum. As controls, patients undergoing ileal resection for other reasons (e.g., right colon cancer) and with healthy terminal ileum were considered.

The following characteristics were registered for CD patients: sex, age, type of surgery, age at diagnosis and age at surgery, smoking status (current, former, never smoked), Montréal classification[96], previous intestinal surgery, treatments at the time of surgery and in the previous year. For controls, only sex, age, ongoing treatments, and reason for surgery were noted.

All patients participating to the study provided written informed consent. The study was approved by the Ethical Committee of Leuven, Belgium (Belgisch Nummer B322201213950-S53684).

2. Biopsy sampling and histology score

Transmural biopsies were obtained from CD patients and controls using 8-mm punch-biopsy needles (Stiefel Dermatology ®, UK) in the presence of an expert pathologist. From the same areas, tissue slices for hematoxylin & eosin (H&E) histology were taken to confirm the macroscopic appearance. A modified score based on the evidence reported in the literature[97-100] was adopted to evaluate the burden of intestinal inflammation and fibrosis (**Table 1**). When a clear difference between inflamed ileum and fibrotic ileum was not reachable, the patient was excluded from the study.

INFLAMMATION SCORE	points
no increased inflammation	0
Inactive chronic inflammation (incl pseudopyloric metaplasia & Paneth cell metaplasia)	1
Mild active chronic inflammation (= neutrophils in lamina propria or epithelium, without crypt abscesses)	2
Moderately active chronic inflammation (= crypt abscess / destruction, or loss of surface epithelium mixed with fibrin)	3
Erosions (= mucosal defect with muscularis mucosae still present)	4
Ulcerations, flat (= mucosal defect without residual muscularis mucosae)	5
Fissuring ulceration (perpendicular, into the deep submucosa or muscularis propria)	6
Fistula / abscess (penetrating the bowel wall)	7

FIBROSIS SCORE	points
no fibrosis	0
Submucosal thickening due to edema	1
Submucosal thickening due to fibrosis	2
Fibrosis in the muscularis propria	3
Fibrosis in the serosa or meso	4
Thickening / splaying of the muscularis mucosae	1
Downward extension of muscularis mucosae	2
Fusion of muscularis mucosae and muscularis propria	3

Table 1: Modified "Inflammation score" and "Fibrosis score" that were used during the study, according to literature evidence.

3. Intestinal fibroblasts isolation

Transmural samples from healthy CD ileum were washed with HBSS buffer and then incubated at 37°C in HBSS solution with 1 mM DTT (Invitrogen®) and 5 mM EDTA (Invitrogen®) on a shaker for 30 minutes at 37 °C to remove the mucosa and the adherent bacteria. After additional washing, a second incubation of 30 minutes at 37°C with 5M EDTA in HBSS followed. The specimen was then cut with sterile scissors and digested with 376 UI of Dispase II (Gibco™), 54 UI of collagenase D (Roche Applied Science®) and 100 UI of DNase I (Sigma-Aldrich®) in DMEM, into the gentleMACS™ Dissociator (Miltenyi Biotec®) for 2 minutes. After incubation on a shaker at 37°C for 30 minutes, the resulting samples were filtered on 70 µm cell strainer and then seeded in T25 flasks in DMEM medium (with 10% FBS, 1% HEPES, 1% sodium pyruvate, 1% pen-strep).

CCD-18Co (normal intestinal fibroblasts from human colon, CRL-1459™) were purchased from ATCC® (Manassas, VA, United States) and cultured in Eagle's Minimum Essential Medium (EMEM) according to manufacturer guidelines. For all experiments, primary fibroblasts and CCD-18Co were starved in low-serum (1%) medium for 24 hours.

4. Immunohistochemistry

Immunohistochemistry (IHC) was performed on formalin-fixed paraffin-embedded ileal sections, from the same areas of biopsy sampling. Automatic machines Leica Bond Max, Leica Autostainer XL and Leica CV5030 (Leica Camera AG®, Germany) were used for staining, counterstaining and slide mounting, respectively. For PAD4 staining, a polyclonal rabbit antibody (final dilution 1:600, Proteintech®, United States) was used. Negative controls stained with secondary antibody only were prepared with the same experimental conditions. Images were acquired with BX41 microscope (Olympus®, Japan) using SC30 colour camera.

5. Immunofluorescence

Immunofluorescence (IF) was performed on ileal sections sampled as described above for IHC. Overnight staining with different primary antibodies on the same slides were done using the MILAN protocol (https://protocolexchange.researchsquare.com/article/nprot-7017/v5) after deparaffinization and dehydration with xylene and ethanol. The following antibodies were used: polyclonal rabbit PAD4 (final dilution 1:4000, Proteintech®, United States), monoclonal mouse vimentin (final dilution 1:300, Agilent®, United States), monoclonal mouse α-SMA (final dilution 1:300, Agilent®, United States), rabbit polyclonal MPO (final dilution 1:200, Abcam®, UK), rabbit polyclonal neutrophil elastase (final dilution 1:1000, Abcam®, UK), rabbit polyclonal H3cit (final dilution 1:400, Abcam®, UK). Each run was scanned with Axio Scan Z1 (Zeiss®, Germany). The slides were then stripped for additional stainings to merge different protein expression. Computational analysis of IF data were performed with custom pipelines coded in R® statistical software, version 4.0.1.

Operetta® CLS™ imager was used to acquire and analyse *in vitro* effect of NETs on intestinal fibroblasts. For this experiment, 96-well microplates were used to seed 3 x10^3 cells. After 24 hours, stimulation or inhibition factors were added. Images were acquired after staining with COL3A1 (final dilution 1:500, NBP1-26547, Novus Biologicals), FAP (final dilution 1:100, AF3715, R&D Systems), Phalloidin-Atto 490LS (final dilution 1:200, 14479-10NMOL, Sigma-Aldrich) and DAPI (final dilution 1:1000, D1306, Invitrogen), and followed by CyTM3 Donkey Anti-Goat IgG (H+L) (final dilution 1:500, 705-165-147, Jackson ImmunoResearch), Alexa Fluor™ 647 Donkey Anti-Mouse IgG (H+L) (final dilution 1:500, A-31571, Invitrogen) and Alexa Fluor™ 488 Donkey Anti-Sheep IgG (H+L) (final dilution 1:500, A-11015, Invitrogen).

6. RNA extraction and quantitative analysis

Transmural samples were processed with TRIzol™ reagent (ThermoFisher Scientific®, United States), according to manufacturer instructions. The corresponding cDNA was retrieved from RNA using the *RevertAid H First Strand cDNA Synthesis Kit* (ThermoFisher Scientific®, United States), following the standard protocol. The real-time quantitative PCR (RT-qPCR) was carried out with *TaqMan® Gene Expression Assays* kits, in duplicates.

In vitro fibroblasts were collected after trypsinization, pelleted, and processed similarly to transmural samples. All primers used for RT-qPCR were bought from Qiagen® (Hilden, Germany).

7. Protein extraction and Western Blot analysis

T-PER reagent (ThermoFisher Scientific®, United States) protocol was used for protein extraction, whose quantification was done with BCA assay. Gel electrophoresis and protein blotting were carried out with Bio-Rad® (California, United States) materials. The following antibodies were used for the experiments: polyclonal rabbit PAD4 (final dilution 1:4000, Proteintech®, United States), monoclonal rabbit phospho-NFkB p65 (Ser536) (final dilution 1:1000, ThermoFisher Scientific®, United States), rabbit polyclonal MyD88 (final dilution 1:5000, Novus Biologicals, United States). Secondary antibodies were diluted 1:5000. Chemoluminescence detection of the proteins was

performed with *SuperSignal™ West Dura Extended Duration Substrate* (ThermoFisher Scientific®, United States) at ImageQuant LAS 4000 Mini ® (GE Healthcare Life Sciences, United States). The ImageJ® software was then used for the final analysis.

8. NETs preparation

Heparinized blood taken from healthy volunteers underwent magnetic separation with *MACSxpress® Whole Blood Neutrophil Isolation Kit* (Miltenyi Biotec®, Germany), according to manufacturer instructions. The resulting neutrophils were then counted in order to seed in six-well plates 1.5 x 10^6 cells in RPMI (Gibco™, ThermoFisher Scientific®, United States) with 2% human serum and 30 nM bafilomycin A1 (Merck®, Germany) to inhibit autophagy. After 30 minutes, cells were incubated for 3.5 hours with the addition of 50 nM phorbol 12-myristate 13-acetate, PMA (Merck®, Germany), to allow the formation of NETs. After removal of supernatant and wash with fresh RPMI, NETs were collected by vigorous pipetting and centrifuged to remove any residual PMA. As last steps, the samples were digested with 4 U/ml Alu-I (ThermoFisher Scientific®, United States) in 1X Tango buffer made in RPMI- HEPES with 0.5% FBS for 20 minutes at 37°C, to allow NETs to detach from debris and dead membranes. NETs quantification and concentration in solution was performed with Quant-iT™ Picogreen dsDNA kit (Thermofisher Scientific®, United States), according to manufacturer instructions.

9. In vitro stimulation and inhibition experiments

In vitro experiments were carried out on primary human intestinal fibroblasts (HIF) from passages 2-5 or CCD18-Co line. HIF were cultured in low-serum DMEM, whereas CCD18-Co line in EMEM, at 37 °C in 5% CO2. All stimulation and inhibition experiments were performed for each patient on the same cell line passage, with cells at subconfluence. Every condition was reproduced at least with triplicates.

For stimulation studies, fibroblast lines were treated with 1 µg/mL NET structures for 24 hours. In inhibition experiments, the biologic effect of NETs was hindered in different ways: 20-minute digestion of NETs with 10 UI/mL DNase I; pre-treatment of neutrophils with 1 µM Thr-Asp-F-amidine trifluoroacetate (TDFA, Merck®, Germany), a selective PAD4 inhibitor, for 15 minutes at 37 °C before PMA stimulation; 1-hour pre-treatment

with 100 µM C29 (MedChemExpress, United States), a potent TLR2 inhibitor. Unstimulated fibroblasts were used as control.

10. RNA sequencing (RNAseq)

For RNAseq, samples were shipped to the service company BGI™ (Beijing Genomics Institute, Shenzhen, China) after quality estimation of RNA using Nanodrop2000™ spectrophotometer (ThermoFisher Scientific®, United States). DNBSEQ™ Sequencing System and its high-throughput platform were used locally and Stranded Poly-A mRNA sequencing service was chosen, with 20 million reads per sample.

In detail, mRNA molecules were purified from total RNA using oligo(dT)-attached magnetic beads, then fragmented into small pieces and added to primers. Afterwards, first-strand cDNA was synthetized and a second-strand cDNA prepared using dUTP. Then, by the "End repair & add A" reaction system, the ends of the double-stranded cDNA were repaired with reverse transcription and A base added to the 3'end. Linker was then connected to A base under enzymatic reaction. PCR amplification was performed and PCR products purified with XP Beads. The double-stranded PCR products were then denatured and circularized by the splint oligo sequence, and the single-strand circle DNA (ssCir DNA) formatted as the final library. The library was amplified with phi29 to make DNA nanoballs (DNBs) that were loaded into the patterned nanoarray, and single end 50 (pair end 100/150) bases reads were generated in the way of combinatorial Probe-Anchor Synthesis (cPAS).

11. Soluble collagen quantification and migration assay (scratch test)

The soluble collagens (types I to V) released by HIF and CCD-18Co were assessed with the Sircol™ Soluble Collagen Assay kit (Biocolor Ltd., UK) by collecting the culture medium after 48-72 hours of exposure to stimulation or inhibition effect. Manufacturer instructions were followed, including the overnight incubation at 4 °C.

The migratory ability of intestinal fibroblasts was tested with a wound healing assay (or scratch test). Briefly, 1 x 10^4 CCD-18Co cells were seeded in a 96-well plate and underwent a scratch with WoundMaker (Sartorius AG, Germany) to create a wound. Cells

were then put into IncuCyte® S3 incubator (Sartorius AG, Germany) and consecutive pictures acquired every 2 hours for 72 hours to assess the differences between the experimental groups.

12. Transfection of human fibroblast cell line

Quiescent CCD-18Co cells were co-transfected with NF-kB and pSV2CAT expression plasmids at the density of 2 x 10^5 cells/well by FuGENE® HD transfection reagent (Promega™, United States), following the manufacturer's instructions. Twenty-four hours after transfection, cells were harvested for luciferase and CAT assay as previously described[101]. Stimulation experiment with NETs and inhibition of the TLR2-associated pathway were carried out. The light emission was read with GloMAX® luminometer (Promega™, United States) after 1 hour of stimulation or inhibition, using CAT activity to normalize the luciferase values. C29 (MedChemExpress®, USA) was used as TLR2 inhibitor at the concentration of 100 μM.

13. Mice

Twelve-week-old female $PAD4^{fl/fl}MRP8^{Cre+}$ and its littermate controls $PAD4^{fl/fl}$ were obtained with a courtesy of *Professor Kim Martinod* (KU Leuven, Belgium)[102]. The mice were subjected to a 12 h light/dark cycle and given free access to the standard rodent chow diet Ssniff® R/M-H (Ssniff Spezialdiäten GmbH, Soest, Germany) and water. All animals were housed in the Laboratory Animal Center at KU Leuven (Leuven, Belgium) and treated in accordance with an Animal Care and Animal Experiments Ethical Committee approval of KU Leuven (protocol P188/2019).

14. Chronic DSS-induced colitis mouse model

Mice were subjected to the administration of 3 cycles of 2.25% (w/v) DSS (MW 36–50 kDa, MP Biomedicals, Santa Ana, CA) to induce chronic colitis and the occurrence of intestinal fibrosis. Each cycle consisted of 7 days of DSS treatment, starting from day 1, followed by a recovery of 14 days with regular drinking water, as already described[103]. Mice were then sacrificed at the end of the experiment (day 63). Mice were monitored

daily for weight loss, stool consistency, and haematochezia. The disease activity index (DAI) was set as the combined score of weight loss (score=0: <1%; 1: ~1%–5%; 2: ~5%–10%; 3: ~10%–20%; 4: >20%), stool blood (score=0: absence; 2: presence; 4: gross bleeding) and stool consistency (score=0: formed and hard; 1: formed but soft; 2: loose stools; 3: mild diarrhoea; 4: gross diarrhoea) as previously described[104], whose total sum could range from 0 to 12 points.

15. Histology and fibrosis analysis

Mice colon were fixed overnight in 4% formaldehyde, embedded in paraffin and cut into 5µm thickness for histological analysis. Picrosirius red staining was completed using a standard protocol. In brief, sections were deparaffinized, incubated with Direct Red 80 (365548-5G, Sigma-Aldrich) in saturated aqueous solution of picric acid (1.3% in water, P6744, Sigma-Aldrich) for 1 h, washed in acetic acid solution, washed in absolute alcohol, cleared with xylene and mounted. Slides were then digitally imaged at 10× (Leica DM2500M) for subsequent analysis. At least two distinct sections were provided for each colon after sacrifice.

The amount of fibrosis was calculated with ImageJ® software, taking into account two different thicknesses: the submucosal red-positive layer (where most of the collagen was produced and accumulated during fibrogenic process), and the muscle layer (as a result of the typical muscularis hyperplasia). Five different measurements in each slide were recorded to reduce the sampling error.

16. Immunofluorescence and collagen quantification

Slides from the same mice after sacrifice were stained for H3cit (with anti-Histone H3, citrulline R2+R8+R17, final dilution 1 µg/mL, Abcam®, UK) and FAP (final dilution 1:100, AF3715, R&D Systems), to show co-localisation of NETs and activated fibroblasts in mice. A similar protocol as for human immunofluorescence was used.

Sircol™ Soluble Collagen Assay kit (Biocolor Ltd., UK) was also utilised on transmural samples as additional confirmation after initial solubilisation of the specimen in a 0.5 M

acid acetic solution with 0.1 mg/mL of pepsin (Merck®, Germany), following manufacturer's instructions.

17. Statistical analysis

For all cases, data are presented as mean ± standard deviation (SD) unless differently specified. One-way or two-way ANOVA was used for parametric comparisons of multiple independent groups, with *post-hoc* T-tests for each independent couple. Paired Student T-test was used for specific cases, when appropriate. All statistics were carried out with GraphPad Prism 8.

For RNAseq, normalization of the raw counts and differential gene expression analysis were performed with DESeq2 package (Version 1.36.0; Bioconductor release 3.15) of R® software (version 4.2.1)[105]. RNAseq data will be soon deposited to be freely available on Gene Expression Omnibus platform upon publication.

The Gene Ontology on the resulting analysed data was performed with ClueGO^{TM} plug-in of Cytoscape software (v. 3.9.1) [106]. The network was created with kappa statistics and with the following settings: medium network specificity (level 3-5), minimum 3 genes (and 4%) for pathway selection, kappa score 0.4, p value < 0.01 with Benjamini-Hochberg correction.

Panther Database (version 17.0 released 2022-02-22) was used to look for potential involved pathways. "Panther pathways" Annotation Data Set was run, using Fisher's exact test with False Discovery Rate (FDR) correction. Only pathways with FDR < 0.05 were considered.

RESULTS

1. Patient inclusions and histopathology evaluation

In total, 15 CD patients with fibrostenotic disease and 14 controls were included in the study. The baseline characteristics of all patients are reported in **Table 2a** and **Table 2b**, respectively. In CD group, patients presented mainly with isolated ileal disease (10/15, 66.6%) and with stenotic phenotype without previous history of penetrating disease (10/15, 66.6%). In one third of cases, this resection was not the first intestinal surgery. In the control group, patients were also mostly female, with a more advanced age due to reasons for surgery (colorectal cancer).

Sex (%, female)	**10/15 (66.6%)**
Age at diagnosis (median, IQR)	29 (22-45)
Age at surgery (median, IQR)	51 (32-65)
Smoking (% yes, active)	1 (6.7%)
Disease location (Montreal Classification, %)	L1 10/15 (66.6%)
	L3 5/15 (33.3%)
Disease behaviour (Montreal Classification, %)	B2 10/15 (66.6%)
	B2-B3 5/15 (33.3%)
Perianal disease (% yes)	2/15 (13.4%)
Drugs at time of surgery	None 6/15 (40%)
	5ASA 1/15 (6.7%)
	Steroids 2/15 (13.4%)
	Anti-TNF 1/15 (6.7%)
	VDZ 1/15 (6.7%)
	UST 3/15 (20.1%)
Previous intestinal resections (% no)	5/15 (33.3%)

a.

Sex (%, female)	**11/14 (78.6%)**
Age at surgery (median, IQR)	68 (61-76)

b.

Table 2: Baseline characteristics of stenotic CD patients undergoing resection **(a.)** and control patients undergoing right hemicolectomy for cancer **(b.)**.

The histopathology analysis showed strong statistical significance to distinguish the different regions (global *p value* < 0.0001), particularly the "inflamed areas" and "fibrotic areas" of CD patients that usually present some overlapping characteristics. Consequently, each sampling from different regions accurately represented either

unaffected, inflamed, or fibrotic tissue. The results are reported in **Figure 7a and Figure 7b** for the *Inflammation score* and the *Fibrosis score*, respectively.

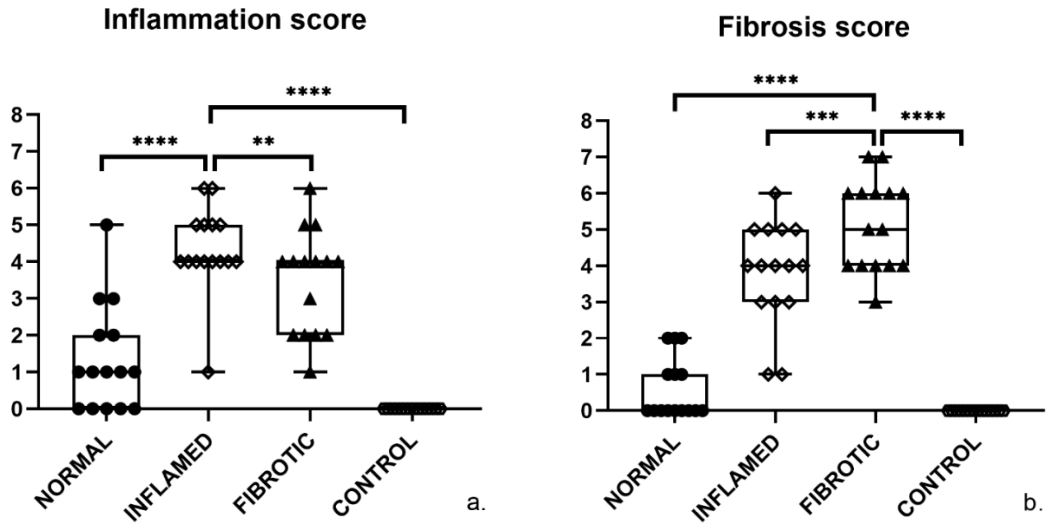

Figure 7: The "inflammation score" (**a.**) was statistically higher in regions that were sampled into or in proximity of large ulcers. On the other hand, the "fibrosis score" (**b.**) was superior in areas collected from stiff and narrow segments. Data are presented for scores performed on H&E slides of 15 CD patients and 14 controls. Statistical significance: ** $p = 0.0044$; *** $p = 0.0002$; **** $p < 0.0001$.

2. PAD4 immunohistochemistry and NETs immunofluorescence

Explorative IHC was performed to show the expression of PAD4 in the ileum of CD patients. No specific staining was shown in normal and fibrotic tissue, whereas a high signal was reported in the nucleus of neutrophils in the inflammatory areas (**Figure 8**). Particularly for the fibrotic samples, no positive staining was found in intestinal fibroblasts, suggesting that the investigation of our hypothesis should have focussed more on the early phases of the fibrotic process instead of when fibrosis is already established.

The multiplex IF analysis confirmed the expression of PAD4 in the nucleus of MPO^+/NE^+ cells (neutrophils) from the inflamed areas (**Figure 9a-f**). Computational analysis demonstrated a strong overlap of citrullinated histone H3 (H3cit) with neutrophil markers and PAD4, defining the presence of NETs. These NETs were mostly found in the inflamed areas with very little expression in the other conditions (**Figure 9g**). In the

proximity of the ulcer bed, groups of aMF (FAP^+ cells) were found close to NETs infiltration, suggesting a possible interaction of neutrophil components with intestinal fibroblasts in the early development of fibrosis (**Figure 10**) as already speculated in the intestine by a recent work of single-cell transcriptomics[84].

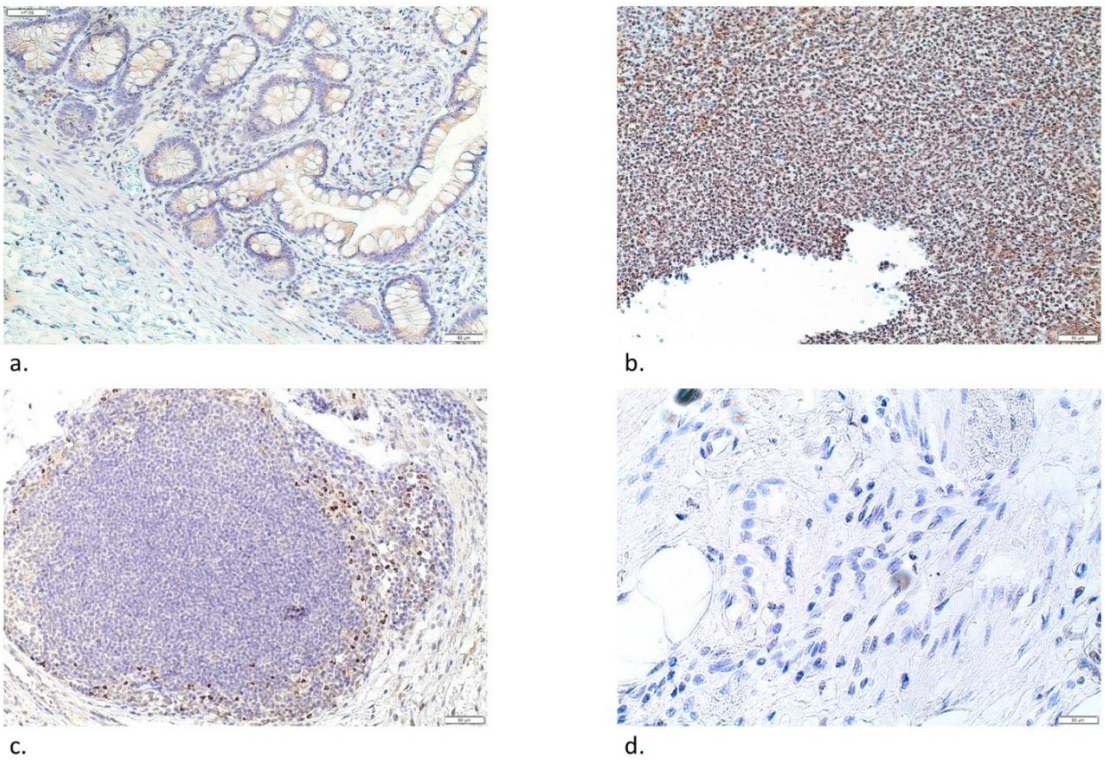

Figure 8: IHC for PAD4. In picture **(a.)**, it is shown an unaffected terminal ileum with no inflammation and no specific staining. Figure **(b.)** shows acute inflammatory infiltration of an ulcer where strong staining in the nucleus of neutrophils is present; in **(c.)**, from the same patient, a detail of a germinative centre of a lymph node, that does not present PAD4 specificity in lymphocytes. In the context of mature intestinal fibrosis, submucosal fibroblasts do not express PAD4 enzyme **(d.)**.

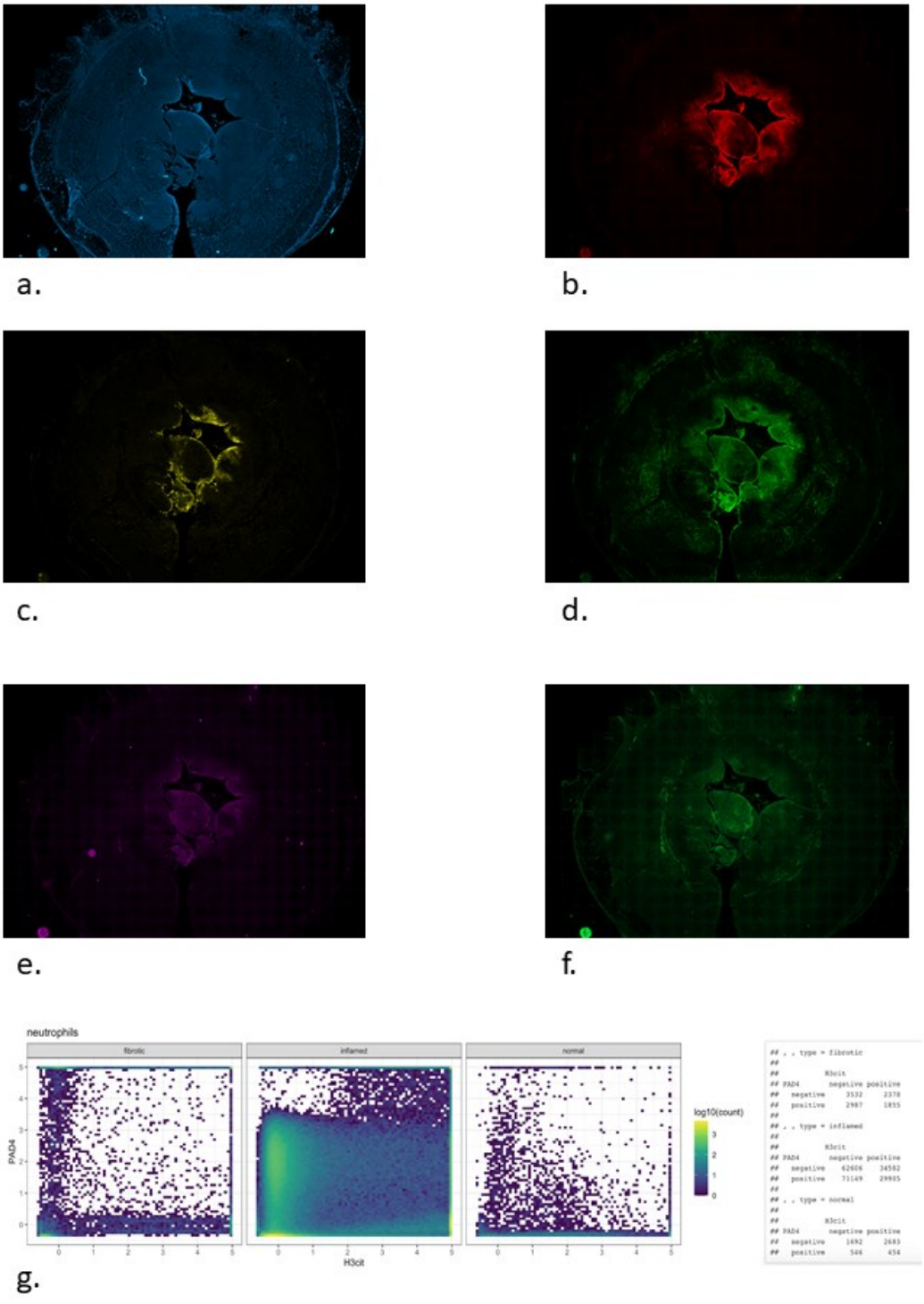

Figure 9: Multiplex IF to identify NETs. In pictures **(a-f)**, the same slide of inflamed ileum was stained for DAPI **(a.)**, PAD4 **(b.)**, H3cit **(c.)**, MPO **(d.)**, NE **(e.)**. Autofluorescence is in **(f.)**. The same process was repeated for unaffected ileum and fibrotic ileum. Overlapping H3cit and PAD4 with neutrophil markers identified NETs within tissues using computational analysis, thus showing upregulation of *NETosis* in inflamed areas (**g.**).

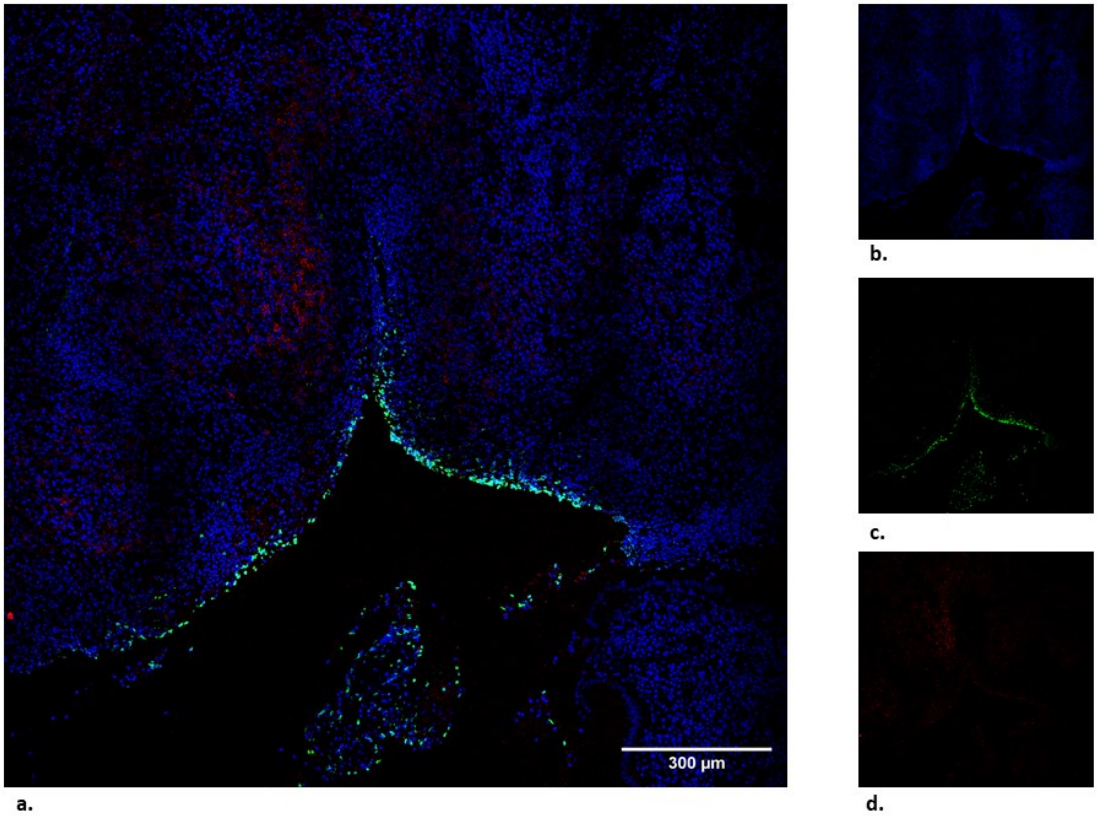

Figure 10: IF imaging of inflamed resected ileum showing co-localisation of H3cit (green) and FAP (red), suggesting potential interaction between NETs and activated intestinal fibroblasts. In (**a.**), it is shown the merged picture; in (**b.**) DAPI, in (**c.**) H3cit, and in (**d.**) FAP.

3. RT-qPCR and Western Blot for PAD4 quantification

The total expression of PAD4 on transmural samples was evaluated at RNA level with RT-qPCR and then confirmed at protein level with WB on the same samples. A significantly higher expression of PAD4 was detected in the inflamed CD group, when compared to all other conditions (**Figure 11**). This result was consistent with histological finding and strengthened the link between PAD4, NETs and intestinal inflammation.

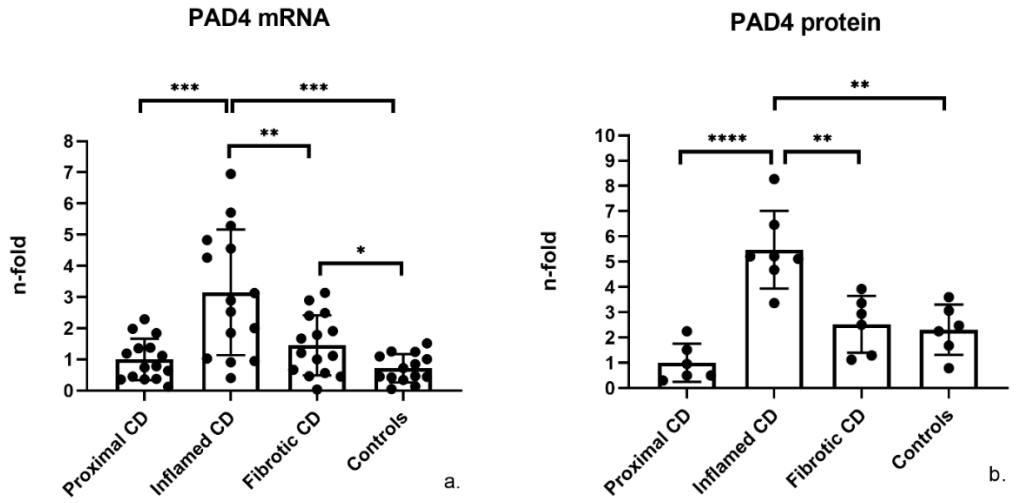

Figure 11: RNA data are shown for 15 CD patients and 14 controls (**a.**), whereas protein analysis of western blots (**c.**) was done on 6 CD and 6 controls (**b.**). Statistical significance: * p = 0.014; ** p < 0.01; *** p < 0.001; **** p < 0.0001.

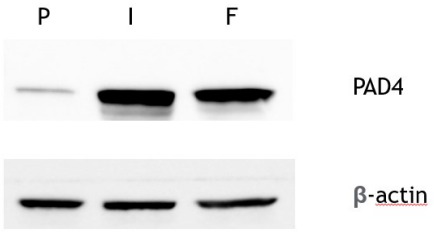

c.

4. Exploratory effect of NETs on intestinal fibroblasts

Despite not being overexpressed in the fibrotic tissue, PAD4-dependendent NETs formation could potentially represent an early trigger of fibroblast activation, thus explaining the reason for very low PAD4 signals in mature fibrotic and stiff tissue. Using a fibrosis panel, we aimed to explore this potential interaction by *in vitro* culturing HIF with NETs for 24 hours. In total, 22 genes were examined with RT-qPCR, i.e., TGFβ, TGFβR1, αSMA, FAP, COL1A1, COL3A1, COL4A1, SNAIL, CCL2, CCL5, CXCL8, CXCR4, MMP1, MMP2, MMP3, MMP7, MMP9, MMP10, TIMP1, TIMP2, TIMP3, and TIMP4.

Of these, TGFβR1, CCL5, CXCL8, CXCR4, MMP3, MMP10, TIMP1 and TIMP4 showed significant increase in stimulated HIF, whereas the others did not show statistical differences between the two conditions (**Figure 12-13**). As initial evidence, we may then speculate that NETs present a triggering signal toward intestinal fibroblasts. In fact, in addition to some metalloproteinases (MMP3, MMP10) and their inhibitors (TIMP1, TIMP4), the "core" receptor of fibrogenesis, TGFβR1, and some key chemokines were also upregulated. For example, CXCL8 (or IL-8) upregulation has shown anti-apoptotic effects in fibroblasts[107], particularly in the ones derived from intestinal strictures[108].

5. Transcriptome of NETs-stimulated fibroblasts

In light of RT-qPCR results, RNAseq of HIF from three patients either stimulated with NETs or left untreated was performed. The subsequent analysis showed that 404 differentially expressed genes (DEG) were present in the comparison, when adjusting for $p < 0.05$ (**Figure 14a**). For example, MMP1, CXCL8, SMAD7, SNAI1, WNT4, and GPR68[109] (that were in the group of DEG) have been strongly linked to the fibrotic process.

We then included the 404 DEG in an algorithm of Cytoscape software to visualize the most significant biological processes involved in the stimulus. Among them, many profibrotic processes were found, such as ECM organization and assembly, positive regulation of collagen metabolic process, TGF-β receptor signalling pathway, positive regulation of SMAD proteins phosphorylation, wound healing, and regulation of cell-cell adhesion (**Figure 14b**). PANTHER Geneontology (http://geneontology.org/) also suggested the Toll-receptor signalling and the TGF-β signalling as two of the main driving pathways (**Table 3**). Therefore, a profibrotic signature of this stimulation was confirmed.

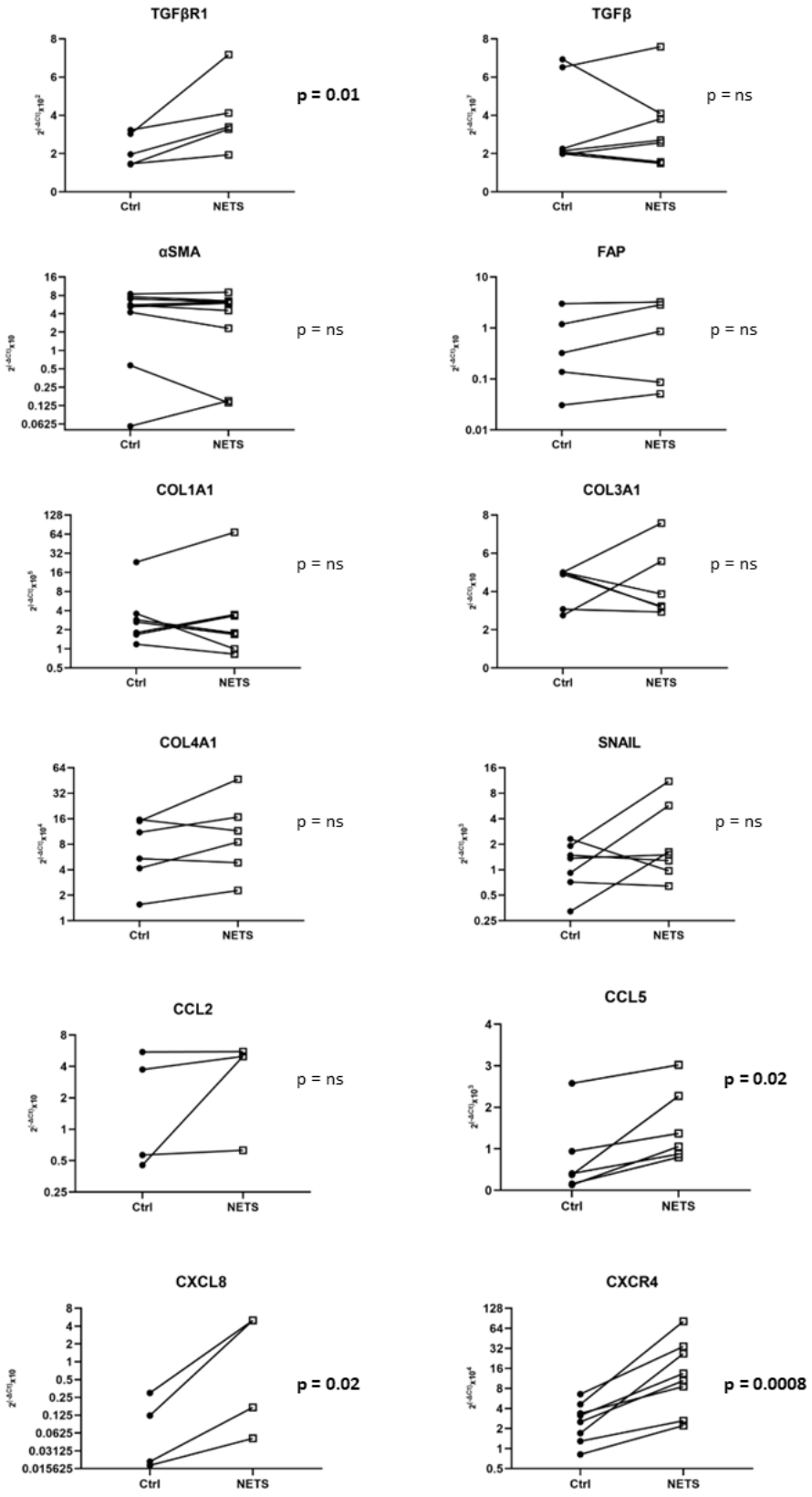

Figure 12: Gene expression of a fibrotic panel in unstimulated fibroblasts (Ctrl) compared to fibroblasts stimulated with NETs (NETS). Paired Student T-test was used for statistical analysis.

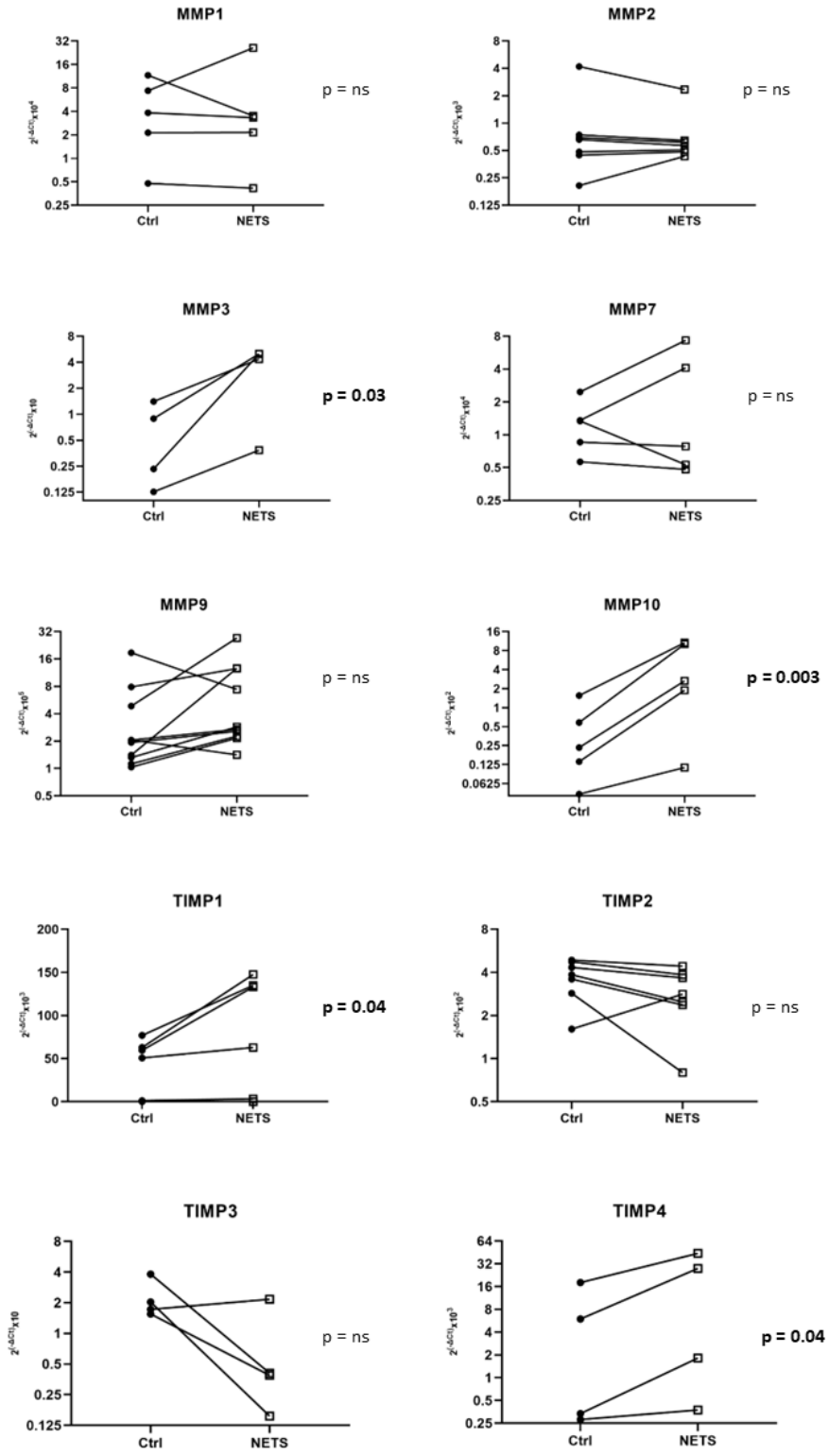

Figure 13: Gene expression of a panel of MMPs and TIMPs in unstimulated fibroblasts (Ctrl) compared to fibroblasts stimulated with NETs (NETS). Paired Student T-test was used for statistical analysis.

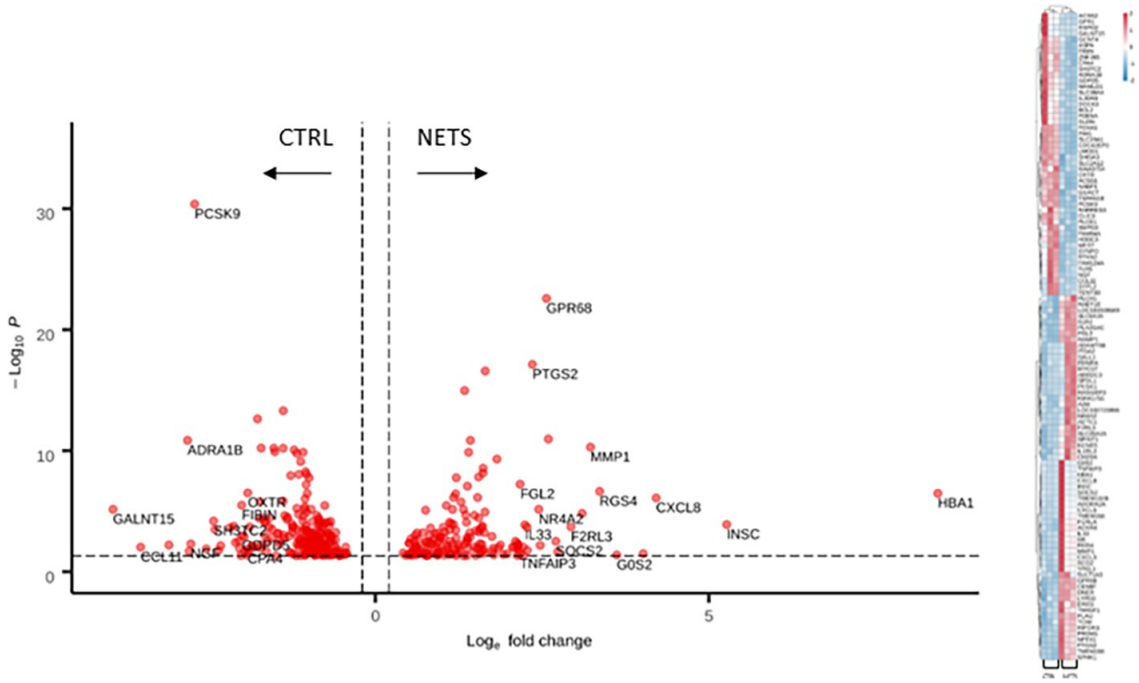

a.

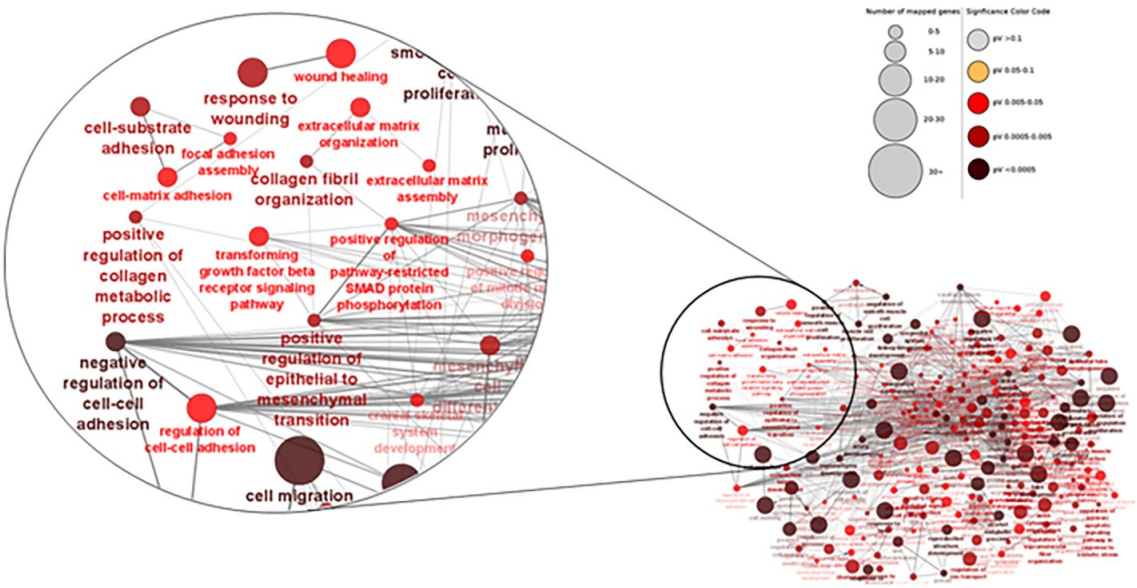

b.

Figure 14: RNAseq representation. In (**a.**), a volcano plot of the 404 DEG between unstimulated fibroblasts (CTRL) and fibroblasts stimulated with NETs (NETS) is shown. The fibrotic signature of these DEG is then highlighted in panel (**b.**), using ClueGo plug-in of Cytoscape.

	Homo sapiens (REF)	upload_1					
PANTHER Pathways	#	#	expected	Fold Enrichment	+/-	raw P value	FDR
TGF-beta signaling pathway	102	7	.83	8.46	+	2.88E-05	1.54E-03
Toll receptor signaling pathway	61	4	.49	8.08	+	1.87E-03	4.27E-02
Endothelin signaling pathway	85	5	.69	7.25	+	8.04E-04	2.14E-02
CCKR signaling map	173	10	1.40	7.13	+	2.37E-06	1.90E-04
Heterotrimeric G-protein signaling pathway-Gq alpha and Go alpha mediated pathway	125	7	1.01	6.90	+	9.76E-05	3.12E-03
Inflammation mediated by chemokine and cytokine signaling pathway	261	10	2.12	4.72	+	7.14E-05	2.86E-03
Unclassified	17971	117	145.77	.80	-	7.00E-09	1.12E-06

Table 3: Representation of the main pathways resulting from the "PANTHER Overrepresentation Test" analysis. Fisher's exact test with False discovery rate (FDR) correction was used.

6. NETs stimulate intestinal fibroblasts through TLR2/NF-kB pathway

Since NETs mainly consist of DNA filaments, we hypothesized that one of the pattern recognition receptor (PRR) pathways may be crucial in the way they activate fibroblasts. As suggested by RNAseq, TLR family may play a direct role on fibroblast activation with NETs components. Therefore, the mRNA expression of all Toll-like receptors (TLR) from TLR1 to TLR10 was tested on intestinal fibroblasts, showing upregulation of TLR2 in fibroblasts stimulated with NETs and downregulation of TLR1 and TLR5 in the same group (**Figure 15**). These data were consistent with the recently demonstrated activation and differentiation of Th-17 lymphocytes through TLR2/Stat3 axis when in presence of NETs [95], and may explain accumulating evidence on TLR signalling and fibrosis, as already mentioned in Chapter 4 of the Introduction "Toll-like receptor (TLR) signalling and fibrosis".

Since NF-kB gene family was differentially regulated at RNAseq, we explored TLR2/MyD88/NF-kB as the main pathway potentially involved in NETs-fibroblast communication. Transfection of CCD-18co fibroblast cell line with NF-kB plasmid resulted in increase of luciferase signal when fibroblasts were exposed to NETs, whereas NF-kB expression was downregulated with C29, a specific TLR2 inhibitor (**Figure 16a**). Accordingly, protein expression of phospho-NF-kB and MyD88 was increased when intestinal fibroblasts were stimulated with NETs, whereas their level was reduced in case of inhibition of the pathway or digestion of NETs DNA filaments with DNase-I (**Figure 16b**).

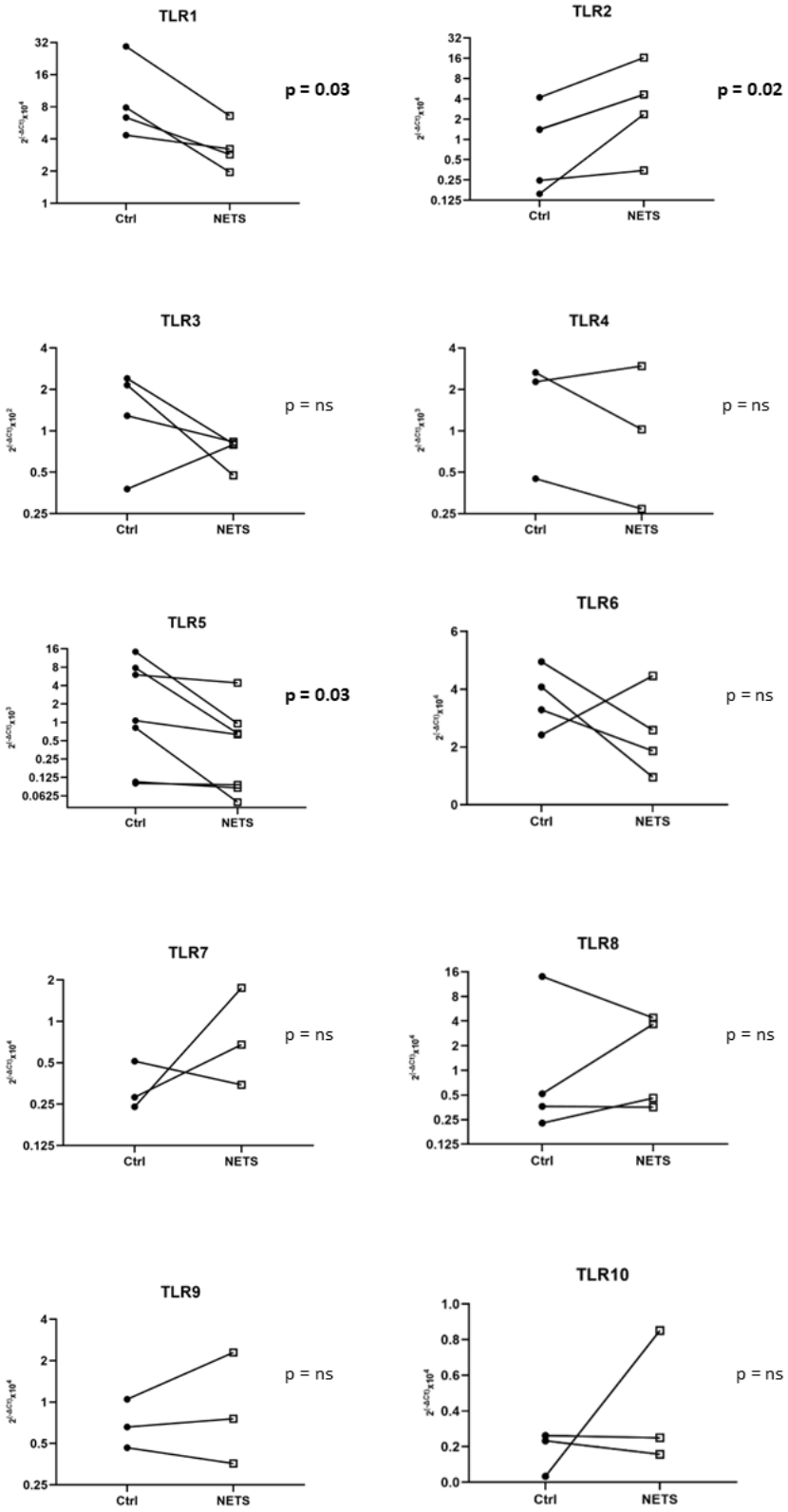

Figure 15: Gene expression of TLRs in unstimulated fibroblasts (Ctrl) compared to fibroblasts stimulated with NETs (NETS). Paired Student T-test was used for statistical analysis.

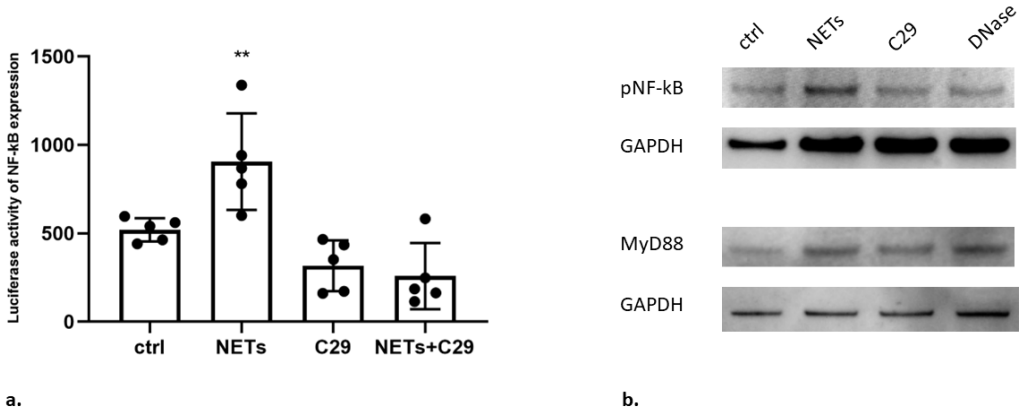

Figure 16: After transfection, NF-kB activity was shown to be significantly upregulated in fibroblasts stimulated with NETs ($p = 0.015$) compared to all controls (**a.**). At protein level, both phospho-NF-kB and MyD88 were upregulated in the group treated with NETs (**b.**).

7. NETs enhance profibrotic properties of fibroblasts

After showing the activation of a profibrotic gene signature, we performed functional experiments to check the variations in the main pre-defined biological activities of fibroblasts, such as collagen production and migration. Although debated, it has been shown that fibroblasts with enhanced profibrotic activity present slower motility[17,22,110]. More in general, it has also been shown that fibroblasts derived from IBD patients present reduced migratory ability than those of healthy individuals[111]. In our scratch test assay, the use of NETs was consistent with the abovementioned literature, thus associated with reduced migratory ability of fibroblasts, resulting in delayed wound healing when compared to control (**Figure 17a-d**). The use of NETs also determined an upregulation of fibroblast proliferation (**Figure 17e**).

Stimulation of HIF with NETs determined an increase in collagen production, tested on medium with SIRCOL® assay (**Figure 17f-g**). Similar results were provided by IF with Operetta® CLS™, where both collagen 3A1 and FAP were upregulated after NETs stimulation (**Figure 17h**). The use of inhibitors of this activity, such as TDFA (PAD4 inhibitor), C29 (TLR2 inhibitor) and DNase-I, was associated with reduced NETs effect.

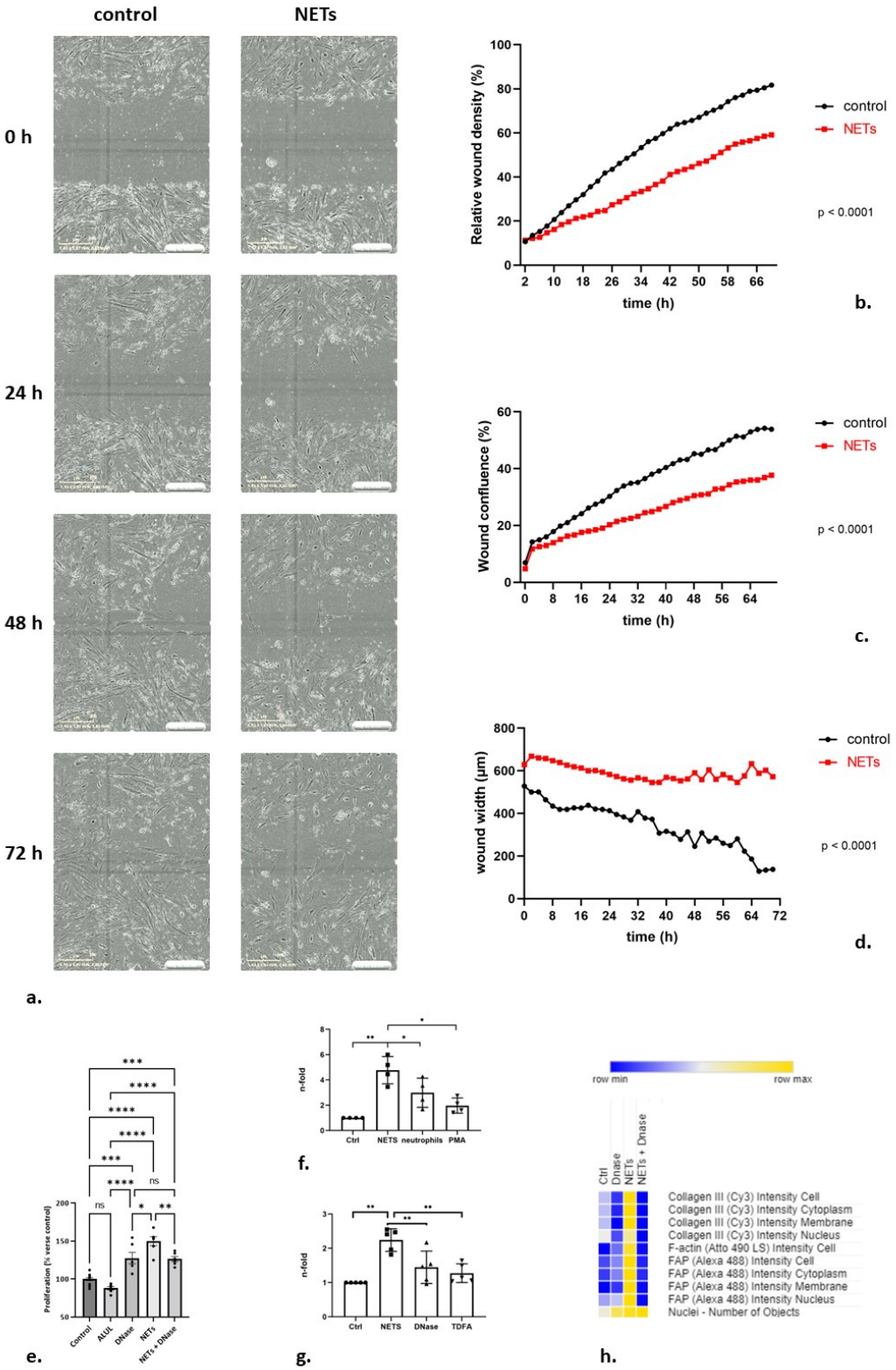

Figure 17: Scratch assay shows a reduced migratory ability and an increased proliferation of fibroblasts treated with NETs (**a-e**). The group of NETs is also the one with the highest release of collagen in the medium (**f-g**), and with higher intracellular expression of collagen and FAP (**h.**). Two-way ANOVA was used for scratch test.

8. PAD4 knocked-out mice are protected from fibrosis

Repeated cycles of DSS colitis simulate chronic intestinal inflammation and the subsequent occurrence of intestinal fibrosis. To validate *in vivo* the role of NETs in the pathogenesis of intestinal fibrosis, we performed a chronic DSS colitis in mice selectively lacking the expression of PAD4 in neutrophils ($PAD4^{fl/fl}MRP8^{Cre+}$).

In total, 11 $PAD4^{fl/fl}MRP8^{Cre+}$ mice and 11 of their related controls ($PAD4^{fl/fl}$) were treated with DSS. During the course of the experiment, 3 mice died in the control group (two after the first DSS cycle, at day 9 and 14, one after the second DSS cycle, at day 35). No mice in the $PAD4^{fl/fl}MRP8^{Cre+}$ group died before sacrifice. From an inflammatory perspective, the DAI was statistically lower in $PAD4^{fl/fl}MRP8^{Cre+}$ mice only during the first recovery phase (day 14 and day 16) (**Figure 18**).

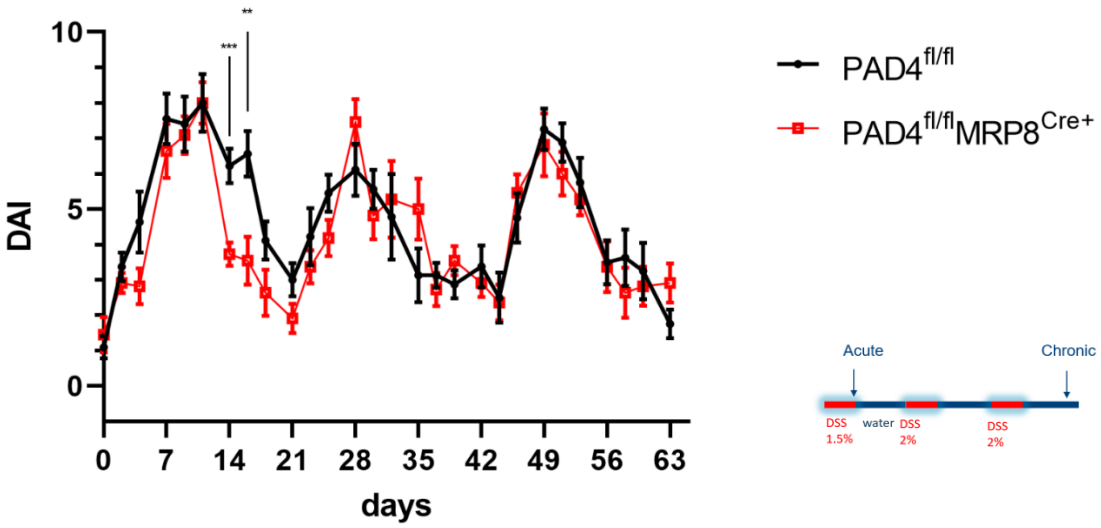

Figure 18: The trend of DAI in the two groups was similar, except for the first recovery phase, and followed the three cycles of DSS and subsequent recoveries (with peak at the end of each acute insult). Comparison between the two groups was performed with Student T test: ** p = 0.054; *** p = 0.0004; for all other time points, p = ns.

Collagen infiltration of the submucosal layer was highlighted with Picrosirius staining of colon slides. The thickness of the submucosal layer was significantly lower in

PAD4$^{fl/fl}$MRP8^{Cre+} mice, suggesting that NETs depletion is associated with a reduced profibrogenic ability (p = 0.04, **Figure 19a-c**). Accordingly, the control group also showed a more prominent hyperplasia of the muscle layer, another key histopathological element of intestinal fibrosis (p = 0.0003, **Figure 19d-f**).

Soluble collagen was assessed with SIRCOL® in transmural colon samples of the two groups, reporting statistically lower collagen amount in PAD4$^{fl/fl}$MRP8^{Cre+} group (p = 0.008, **Figure 20**). As shown in human ileum, the co-localisation of FAP^{+} fibroblasts and H3cit was also present in the colon of PAD4$^{fl/fl}$ mice, whereas FAP and H3cit were downregulated in the group of PAD4$^{fl/fl}$MRP8^{Cre} (**Figure 21**).

Additional analyses at RNA and protein levels on mice samples are ongoing to confirm our findings.

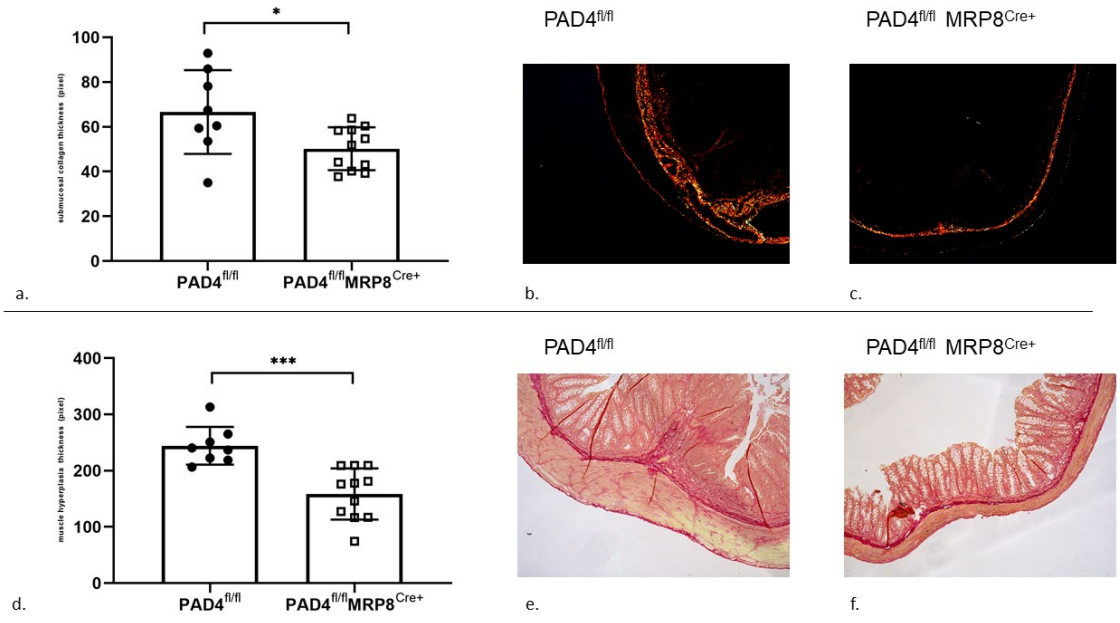

Figure 19: Histological analysis of the colon after sacrifice. PAD4$^{fl/fl}$MRP8^{Cre+} mice undergoing chronic inflammation presented less collagen infiltration in the submucosal layer as shown with Picrosirius red (**a-c**), and lower amount of muscle hyperplasia than controls (**d-f**).

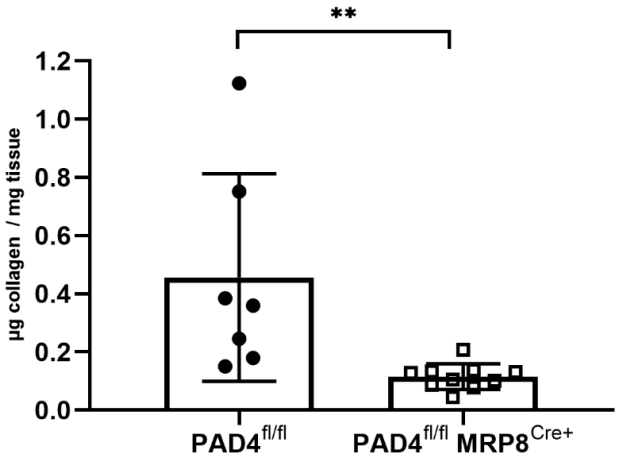

Figure 20: Deletion of NETs formation is associated with reduced accumulation of soluble collagen in transmural colon samples, assessed with SIRCOL®.

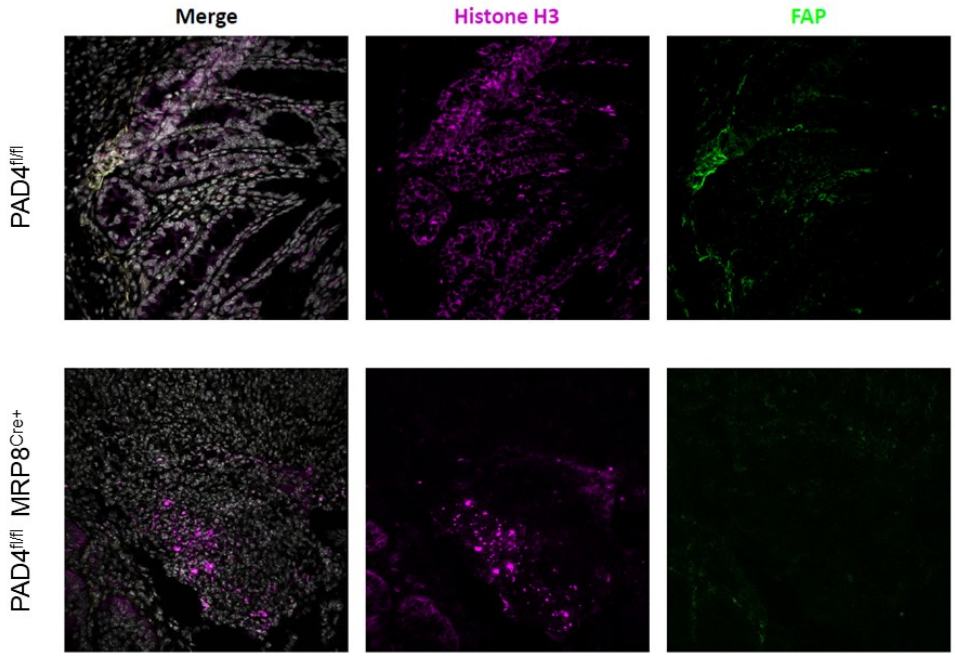

Figure 21: Co-localisation of FAP and H3cit was observed in colon of PAD4$^{fl/fl}$ mice, similar to inflamed human ileum. In the group where PAD4-dependent production of NETs was hampered, FAP was also reduced.

DISCUSSION

Neutrophils are the first cells of innate immunity to react to tissue damage, infiltrating ulcerated areas and releasing NETs with the final intent to repair the wound[112]. Neutrophil activation and NETs formation is associated with production and release of various proteases and matrix metalloproteinases that prolong inflammation and delay wound healing. The digestion of ECM may indirectly increase the recruitment of aMF at the site of the wound and promote the formation of a hypertrophic scar. Co-localisation of NETs and activated fibroblasts was already shown in the lung and in skin scar tissue[69], speculating that this interaction may be broad and not tissue-specific. In our work, groups of aMF (FAP^+ cells) were indeed found close to NETs infiltration in the proximity of the ulcer bed both in human and mouse intestine, suggesting a possible interaction of neutrophils and fibroblasts in the early development of intestinal fibrosis. The potential link between these two cell lines has already been shown in the intestine by a recent work of single-cell transcriptomics[84], and might help tackle the process of fibrogenesis in its early phases avoiding (or at least delaying) downstream cascades.

One could argue that neutrophil elastase, one of the main granules of neutrophils that is also included in NETs, has been already shown to promote myofibroblast proliferation and differentiation in lung fibrosis[113]. However, we have demonstrated with this study that collagen production is reduced with DNase-I, thus confirming that the DNA traps of NETs are fundamental in inducing a profibrotic profile. Moreover, the production of collagen by intestinal fibroblasts is also hampered with the use of TLR2 inhibitors, suggesting that other NETs components such as histones are necessary to activate this receptor. Consequently, we may say that NETs exert their function on fibroblasts through the TLR2/MyD88 axis.

The signature gene of fibroblast activation and profibrotic differentiation of intestinal fibroblasts is to be considered FAP, as already explained in the first pages of this manuscript. In our data, we found that NETs are able to increase FAP production of intestinal fibroblasts, thus upregulating their fibrotic functions. Increased expression of FAP and collagens in fibroblasts activated with NETs was also recently reported in a model of fibrous thrombus formation, suggesting that NETs may be the upstream stimulus of TGFβ signalling[75]. Therefore, targeting their acute activation could

potentially avoid chronic perpetuation of fibroblast activity. On the other hand, we did not find evidence that NETs trigger the transition of fibroblasts into myofibroblast, since αSMA levels do not increase in this environment, consistent with the work of Heuer *et al.*[82] on the mechanisms of wound healing in mice.

With our data, we have also demonstrated that NETs reduce the migratory ability of fibroblasts, resulting in delayed wound healing. Although this is in contrast with published evidence on lung fibroblasts where the motility was instead increasing with NETs[69], it has been shown in many other papers that fibroblasts with higher fibrotic activity present slower migration rate[17,22,110]. Specifically in the context of IBD, it has also been reported that fibroblasts derived from IBD patients present reduced migratory ability than those of healthy individuals[111]. Therefore, our results are consistent with most of the published literature in the field of intestinal fibrosis.

In our chronic DSS model, we did not find strong statistical difference between PAD4-knockout ($PAD4^{fl/fl}MRP8^{Cre+}$) and wild-type mice ($PAD4^{fl/fl}$) regarding the inflammatory score (i.e., DAI). The reason for this result may be two-fold. First, a lower concentration of DSS (2.25%) was used in our model during chronic inflammation compared to the one routinely used for acute DSS colitis (3-4%), as reported in other studies in the same context where a protective effect of PAD4 inhibition was observed[58,66,114]. Second, our study is the first that focusses on selective PAD4 inhibition in neutrophils, whereas either a global PAD4 inhibition or a fully PAD4-knockout mouse was proposed in all other papers. In addition, a similar work of acute DSS colitis failed to show improved body weight, stool consistency or colon length in the arms of mice treated with PAD4 inhibitors, but only reported lower concentration of extracellular DNA in the plasma[115]. Moreover, all three deaths observed during our experiment were in the group with preserved PAD4 expression and NETs formation, suggesting a potential protective role of PAD4 inhibition. Despite this, DAI activity was not our primary endpoint of the experiment. In terms of intestinal fibrosis, we have shown that PAD4-knockout mice presented a downregulation of this process, although final confirmations are needed at RNA and protein levels.

Similar to our findings, in a mouse model of post-epidural fibrosis, it has been reported that NETs activation of profibrotic macrophages was dependent on NE and on the NF-kB/Smad3 pathways since these two downstream genes were upregulated during the

wound healing process[72]. In a bleomycin-induced mouse model of lung fibrosis, PAD4-knockout mice showed significantly reduced levels of collagen 1A1, elastin, fibronectin and CTGF, but only numerically lower levels of ACTA2 and TGFβ1[73]. Moreover, in the same work the authors also reported that bleomycin-induced NETs formation was not completely inhibited in PAD4-KO mice, suggesting that mechanisms independent from PAD4 may contribute to NETs formation, such as autophagy and activation of NE/MPO[116,117].

Our work is unique because only a specific cell line of the *in vivo* confirmatory experiments was PAD4-knockout targeted, i.e., neutrophils, whereas in all other papers in literature a more generic silencing of PAD4 applied to all cells[58,66,73,74,114], reducing the relevance of those data in terms of NETs specificity of their findings.

A potential limitation to our study is that unknown mechanisms independent from PAD4 blocking *NETosis* may exist[116,117], since residual NETs were still visible also in our PAD4-knockout model. However, the ability to block the vast majority of the phenomenon of *NETosis* can be considered sufficient to mitigate the fibrotic process. In addition, we did not show a direct visualization of NET-TLR engagement, opening the possibility of indirect effect rather than direct link between these two components. Nonetheless, the prompt activation (within 1 hour) of TLR2 signal upon NETs stimulation points toward a primary effect.

In conclusion, we have shown that blocking PAD4 and the subsequent formation of NETs downregulates intestinal fibrosis. Together with the evidence on intestinal inflammation, targeting this enzyme may represent a valuable option to tackle both intestinal inflammation and fibrosis. Further research is needed in this field to confirm our findings.

ACKNOWLEDGMENTS

This work has been partially supported by the European Crohn's and Colitis Organisation (ECCO) with the "ECCO Grant 2020", held by Dr. Gabriele Dragoni for the years 2020-2021.

REFERENCES

1. Torres J, Mehandru S, Colombel JF, Peyrin-Biroulet L. Crohn's disease. *Lancet* 2017;**389**:1741-55.
2. de Souza HS, Fiocchi C. Immunopathogenesis of ibd: Current state of the art. *Nat Rev Gastroenterol Hepatol* 2016;**13**:13-27.
3. Rieder F, Fiocchi C, Rogler G. Mechanisms, management, and treatment of fibrosis in patients with inflammatory bowel diseases. *Gastroenterology* 2017;**152**:340-50.e6.
4. Rieder F, Latella G, Magro F*, et al.* European crohn's and colitis organisation topical review on prediction, diagnosis and management of fibrostenosing crohn's disease. *J Crohns Colitis* 2016;**10**:873-85.
5. Steiner CA, Berinstein JA, Louissaint J*, et al.* Biomarkers for the prediction and diagnosis of fibrostenosing crohn's disease: A systematic review. *Clinical gastroenterology and hepatology : the official clinical practice journal of the American Gastroenterological Association* 2021.
6. Johnson LA, Luke A, Sauder K*, et al.* Intestinal fibrosis is reduced by early elimination of inflammation in a mouse model of ibd: Impact of a "Top-down" Approach to intestinal fibrosis in mice. *Inflamm Bowel Dis* 2012;**18**:460-71.
7. Latella G, Di Gregorio J, Flati V, Rieder F, Lawrance IC. Mechanisms of initiation and progression of intestinal fibrosis in ibd. *Scand J Gastroenterol* 2015;**50**:53-65.
8. Hünerwadel A, Fagagnini S, Rogler G*, et al.* Severity of local inflammation does not impact development of fibrosis in mouse models of intestinal fibrosis. *Sci Rep* 2018;**8**:15182.
9. Zhao JF, Ling FM, Li JR*, et al.* Role of non-inflammatory factors in intestinal fibrosis. *J Dig Dis* 2020;**21**:315-8.
10. Gordon IO, Bettenworth D, Bokemeyer A*, et al.* International consensus to standardise histopathological scoring for small bowel strictures in crohn's disease. *Gut* 2022;**71**:479-86.
11. Alfredsson J, Wick MJ. Mechanism of fibrosis and stricture formation in crohn's disease. *Scandinavian Journal of Immunology* 2020;**92**.
12. Rittié L. Method for picrosirius red-polarization detection of collagen fibers in tissue sections. *Methods Mol Biol* 2017;**1627**:395-407.
13. Rieder F, Karrasch T, Ben-Horin S*, et al.* Results of the 2nd scientific workshop of the ecco (iii): Basic mechanisms of intestinal healing. *J Crohns Colitis* 2012;**6**:373-85.
14. Burke JP, Mulsow JJ, O'Keane C*, et al.* Fibrogenesis in crohn's disease. *Am J Gastroenterol* 2007;**102**:439-48.
15. D'Haens G, Rieder F, Feagan BG*, et al.* Challenges in the pathophysiology, diagnosis, and management of intestinal fibrosis in inflammatory bowel disease. *Gastroenterology* 2022;**162**:26-31.
16. Rovedatti L, Di Sabatino A, Knowles CH*, et al.* Fibroblast activation protein expression in crohn's disease strictures. *Inflamm Bowel Dis* 2011;**17**:1251-3.

17. Truffi M, Sorrentino L, Monieri M*, et al.* Inhibition of fibroblast activation protein restores a balanced extracellular matrix and reduces fibrosis in crohn's disease strictures ex vivo. *Inflamm Bowel Dis* 2018;**24**:332-45.
18. Pariente B, Hu S, Bettenworth D*, et al.* Treatments for crohn's disease-associated bowel damage: A systematic review. *Clin Gastroenterol Hepatol* 2019;**17**:847-56.
19. Duffield JS, Lupher M, Thannickal VJ, Wynn TA. Host responses in tissue repair and fibrosis. *Annu Rev Pathol* 2013;**8**:241-76.
20. Wynn TA, Ramalingam TR. Mechanisms of fibrosis: Therapeutic translation for fibrotic disease. *Nat Med* 2012;**18**:1028-40.
21. Ramani K, Biswas PS. Interleukin-17: Friend or foe in organ fibrosis. *Cytokine* 2019;**120**:282-8.
22. Di Sabatino A, Jackson CL, Pickard KM*, et al.* Transforming growth factor beta signalling and matrix metalloproteinases in the mucosa overlying crohn's disease strictures. *Gut* 2009;**58**:777-89.
23. Moore CS, Crocker SJ. An alternate perspective on the roles of timps and mmps in pathology. *Am J Pathol* 2012;**180**:12-6.
24. Yun SM, Kim SH, Kim EH. The molecular mechanism of transforming growth factor-β signaling for intestinal fibrosis: A mini-review. *Front Pharmacol* 2019;**10**:162.
25. Latella G, Rogler G, Bamias G*, et al.* Results of the 4th scientific workshop of the ecco (i): Pathophysiology of intestinal fibrosis in ibd. *Journal of Crohn's and Colitis* 2014;**8**:1147-65.
26. D'Alessio S, Ungaro F, Noviello D*, et al.* Revisiting fibrosis in inflammatory bowel disease: The gut thickens. *Nat Rev Gastroenterol Hepatol* 2022;**19**:169-84.
27. Zhao Z, Cheng W, Qu W, Shao G, Liu S. Antibiotic alleviates radiation-induced intestinal injury by remodeling microbiota, reducing inflammation, and inhibiting fibrosis. *ACS Omega* 2020;**5**:2967-77.
28. Rieder F, Kessler S, Sans M, Fiocchi C. Animal models of intestinal fibrosis: New tools for the understanding of pathogenesis and therapy of human disease. *Am J Physiol Gastrointest Liver Physiol* 2012;**303**:G786-801.
29. Hinz B. Tissue stiffness, latent tgf-beta1 activation, and mechanical signal transduction: Implications for the pathogenesis and treatment of fibrosis. *Curr Rheumatol Rep* 2009;**11**:120-6.
30. Wells RG. The role of matrix stiffness in regulating cell behavior. *Hepatology* 2008;**47**:1394-400.
31. Ikushima H, Miyazono K. Tgfbeta signalling: A complex web in cancer progression. *Nat Rev Cancer* 2010;**10**:415-24.
32. Pizarro TT, Pastorelli L, Bamias G*, et al.* Samp1/yitfc mouse strain: A spontaneous model of crohn's disease-like ileitis. *Inflamm Bowel Dis* 2011;**17**:2566-84.
33. Breynaert C, Dresselaers T, Perrier C*, et al.* Unique gene expression and mr t2 relaxometry patterns define chronic murine dextran sodium sulphate colitis as a model for connective tissue changes in human crohn's disease. *PLoS One* 2013;**8**:e68876.
34. Lawrance IC, Wu F, Leite AZ*, et al.* A murine model of chronic inflammation-induced intestinal fibrosis down-regulated by antisense nf-kappa b. *Gastroenterology* 2003;**125**:1750-61.

35. Grassl GA, Valdez Y, Bergstrom KS, Vallance BA, Finlay BB. Chronic enteric salmonella infection in mice leads to severe and persistent intestinal fibrosis. *Gastroenterology* 2008;**134**:768-80.
36. Small CL, Reid-Yu SA, McPhee JB, Coombes BK. Persistent infection with crohn's disease-associated adherent-invasive escherichia coli leads to chronic inflammation and intestinal fibrosis. *Nat Commun* 2013;**4**:1957.
37. Simmons JG, Pucilowska JB, Keku TO, Lund PK. Igf-i and tgf-beta1 have distinct effects on phenotype and proliferation of intestinal fibroblasts. *Am J Physiol Gastrointest Liver Physiol* 2002;**283**:G809-18.
38. Morrissey PJ, Charrier K, Braddy S, Liggitt D, Watson JD. Cd4+ t cells that express high levels of cd45rb induce wasting disease when transferred into congenic severe combined immunodeficient mice. Disease development is prevented by cotransfer of purified cd4+ t cells. *J Exp Med* 1993;**178**:237-44.
39. Gervaz P, Morel P, Vozenin-Brotons MC. Molecular aspects of intestinal radiation-induced fibrosis. *Curr Mol Med* 2009;**9**:273-80.
40. Rigby RJ, Hunt MR, Scull BP*, et al.* A new animal model of postsurgical bowel inflammation and fibrosis: The effect of commensal microflora. *Gut* 2009;**58**:1104-12.
41. Spencer DM, Veldman GM, Banerjee S, Willis J, Levine AD. Distinct inflammatory mechanisms mediate early versus late colitis in mice. *Gastroenterology* 2002;**122**:94-105.
42. Latella G, Vetuschi A, Sferra R*, et al.* Smad3 loss confers resistance to the development of trinitrobenzene sulfonic acid-induced colorectal fibrosis. *Eur J Clin Invest* 2009;**39**:145-56.
43. Xiong S, Whitehurst CE, Li L*, et al.* Reverse translation approach generates a signature of penetrating fibrosis in crohn's disease that is associated with anti-tnf response. *Gut* 2022;**71**:1289-301.
44. Bamias G, Pizarro TT, Cominelli F. Immunological regulation of intestinal fibrosis in inflammatory bowel disease. *Inflamm Bowel Dis* 2022;**28**:337-49.
45. Estrada HQ, Patel S, Rabizadeh S*, et al.* Development of a personalized intestinal fibrosis model using human intestinal organoids derived from induced pluripotent stem cells. *Inflamm Bowel Dis* 2022;**28**:667-79.
46. Papayannopoulos V. Neutrophil extracellular traps in immunity and disease. *Nat Rev Immunol* 2018;**18**:134-47.
47. Sørensen OE, Borregaard N. Neutrophil extracellular traps - the dark side of neutrophils. *J Clin Invest* 2016;**126**:1612-20.
48. Denning NL, Aziz M, Gurien SD, Wang P. Damps and nets in sepsis. *Front Immunol* 2019;**10**:2536.
49. Jorch SK, Kubes P. An emerging role for neutrophil extracellular traps in noninfectious disease. *Nat Med* 2017;**23**:279-87.
50. Brinkmann V, Reichard U, Goosmann C*, et al.* Neutrophil extracellular traps kill bacteria. *Science* 2004;**303**:1532-5.

51. Slaba I, Wang J, Kolaczkowska E, *et al.* Imaging the dynamic platelet-neutrophil response in sterile liver injury and repair in mice. *Hepatology* 2015;**62**:1593-605.
52. Dragoni G, De Hertogh G, Vermeire S. The role of citrullination in inflammatory bowel disease: A neglected player in triggering inflammation and fibrosis? *Inflamm Bowel Dis* 2021;**27**:134-44.
53. Dos Santos Ramos A, Viana GCS, de Macedo Brigido M, Almeida JF. Neutrophil extracellular traps in inflammatory bowel diseases: Implications in pathogenesis and therapeutic targets. *Pharmacol Res* 2021;**171**:105779.
54. Bennike TB, Carlsen TG, Ellingsen T, *et al.* Neutrophil extracellular traps in ulcerative colitis: A proteome analysis of intestinal biopsies. *Inflamm Bowel Dis* 2015;**21**:2052-67.
55. Gottlieb Y, Elhasid R, Berger-Achituv S, *et al.* Neutrophil extracellular traps in pediatric inflammatory bowel disease. *Pathol Int* 2018;**68**:517-23.
56. Li T, Wang C, Liu Y, *et al.* Neutrophil extracellular traps induce intestinal damage and thrombotic tendency in inflammatory bowel disease. *J Crohns Colitis* 2020;**14**:240-53.
57. Lehmann T, Schallert K, Vilchez-Vargas R, *et al.* Metaproteomics of fecal samples of crohn's disease and ulcerative colitis. *J Proteomics* 2019;**201**:93-103.
58. Dinallo V, Marafini I, Di Fusco D, *et al.* Neutrophil extracellular traps sustain inflammatory signals in ulcerative colitis. *J Crohns Colitis* 2019;**13**:772-84.
59. Angelidou I, Chrysanthopoulou A, Mitsios A, *et al.* Redd1/autophagy pathway is associated with neutrophil-driven il-1β inflammatory response in active ulcerative colitis. *J Immunol* 2018;**200**:3950-61.
60. Schroder AL, Chami B, Liu Y, *et al.* Neutrophil extracellular trap density increases with increasing histopathological severity of crohn's disease. *Inflamm Bowel Dis* 2022;**28**:586-98.
61. Chumanevich AA, Causey CP, Knuckley BA, *et al.* Suppression of colitis in mice by cl-amidine: A novel peptidylarginine deiminase inhibitor. *Am J Physiol Gastrointest Liver Physiol* 2011;**300**:G929-38.
62. Chami B AG, Schroder A, San Gabriel P, Witting P. The role of myeloperoxidase and neutrophil extracellular traps in the pathogenesis of inflammatory bowel disease. 2021: DOI: https://doi.org/10.1053/j.gastro.2021.01.044.
63. Cao D, Qian K, Zhao Y, *et al.* Association of neutrophil extracellular traps with fistula healing in patients with complex perianal fistulising crohn's disease. *J Crohns Colitis* 2022.
64. He Z, Si Y, Jiang T, *et al.* Phosphotidylserine exposure and neutrophil extracellular traps enhance procoagulant activity in patients with inflammatory bowel disease. *Thromb Haemost* 2016;**115**:738-51.
65. Cao M YM, Zhang Y, Tong D, et al. Neutrophil extracellular traps exacerbate inflammatory responses and thrombotic tendency in both a murine colitis model and patients with inflammatory bowel disease. Blood, December 2017: 994.
66. Leppkes M, Lindemann A, Gößwein S, *et al.* Neutrophils prevent rectal bleeding in ulcerative colitis by peptidyl-arginine deiminase-4-dependent immunothrombosis. *Gut* 2022;**71**:2414-29.
67. Gorschlüter M, Mey U, Strehl J, *et al.* Neutropenic enterocolitis in adults: Systematic analysis of evidence quality. *Eur J Haematol* 2005;**75**:1-13.

68. Wilgus TA, Roy S, McDaniel JC. Neutrophils and wound repair: Positive actions and negative reactions. *Adv Wound Care (New Rochelle)* 2013;**2**:379-88.
69. Chrysanthopoulou A, Mitroulis I, Apostolidou E*, et al.* Neutrophil extracellular traps promote differentiation and function of fibroblasts. *J Pathol* 2014;**233**:294-307.
70. Zhang S, Jia X, Zhang Q*, et al.* Neutrophil extracellular traps activate lung fibroblast to induce polymyositis-related interstitial lung diseases via tlr9-mir-7-smad2 pathway. *J Cell Mol Med* 2020;**24**:1658-69.
71. Martinod K, Witsch T, Erpenbeck L*, et al.* Peptidylarginine deiminase 4 promotes age-related organ fibrosis. *J Exp Med* 2017;**214**:439-58.
72. Jin Z, Sun J, Song Z*, et al.* Neutrophil extracellular traps promote scar formation in post-epidural fibrosis. *NPJ Regen Med* 2020;**5**:19.
73. Suzuki M, Ikari J, Anazawa R*, et al.* Pad4 deficiency improves bleomycin-induced neutrophil extracellular traps and fibrosis in mouse lung. *Am J Respir Cell Mol Biol* 2020;**63**:806-18.
74. Kuyl EV, Shu F, Sosa BR*, et al.* Inhibition of pad4 mediated neutrophil extracellular traps prevents fibrotic osseointegration failure in a tibial implant murine model : An animal study. *Bone Joint J* 2021;**103-B**:135-44.
75. Sharma S, Hofbauer TM, Ondracek AS*, et al.* Neutrophil extracellular traps promote fibrous vascular occlusions in chronic thrombosis. *Blood* 2021;**137**:1104-16.
76. Wang W, Liu Z, Zhang Y*, et al.* Benzyl butyl phthalate (bbp) induces lung injury and fibrosis through neutrophil extracellular traps. *Environ Pollut* 2022;**309**:119743.
77. Negreros M, Flores-Suárez LF. A proposed role of neutrophil extracellular traps and their interplay with fibroblasts in anca-associated vasculitis lung fibrosis. *Autoimmun Rev* 2021;**20**:102781.
78. Frangou E, Chrysanthopoulou A, Mitsios A*, et al.* Redd1/autophagy pathway promotes thromboinflammation and fibrosis in human systemic lupus erythematosus (sle) through nets decorated with tissue factor (tf) and interleukin-17a (il-17a). *Ann Rheum Dis* 2019;**78**:238-48.
79. Herrick S, Ashcroft G, Ireland G*, et al.* Up-regulation of elastase in acute wounds of healthy aged humans and chronic venous leg ulcers are associated with matrix degradation. *Lab Invest* 1997;**77**:281-8.
80. Wong SL, Demers M, Martinod K*, et al.* Diabetes primes neutrophils to undergo netosis, which impairs wound healing. *Nat Med* 2015;**21**:815-9.
81. Yang S, Gu Z, Lu C*, et al.* Neutrophil extracellular traps are markers of wound healing impairment in patients with diabetic foot ulcers treated in a multidisciplinary setting. *Adv Wound Care (New Rochelle)* 2020;**9**:16-27.
82. Heuer A, Stiel C, Elrod J*, et al.* Therapeutic targeting of neutrophil extracellular traps improves primary and secondary intention wound healing in mice. *Front Immunol* 2021;**12**:614347.
83. Wier E, Asada M, Wang G*, et al.* Neutrophil extracellular traps impair regeneration. *J Cell Mol Med* 2021;**25**:10008-19.
84. Friedrich M, Pohin M, Jackson MA*, et al.* Il-1-driven stromal-neutrophil interactions define a subset of patients with inflammatory bowel disease that does not respond to therapies. *Nat Med* 2021;**27**:1970-81.

85. Sabbatini M, Magnelli V, Renò F. Netosis in wound healing: When enough is enough. *Cells* 2021;**10**.
86. Bautista-Hernández LA, Gómez-Olivares JL, Buentello-Volante B, Bautista-de Lucio VM. Fibroblasts: The unknown sentinels eliciting immune responses against microorganisms. *Eur J Microbiol Immunol (Bp)* 2017;**7**:151-7.
87. Strippoli R, Moreno-Vicente R, Battistelli C*, et al.* Molecular mechanisms underlying peritoneal emt and fibrosis. *Stem Cells Int* 2016;**2016**:3543678.
88. Arslan F, Smeets MB, Riem Vis PW*, et al.* Lack of fibronectin-eda promotes survival and prevents adverse remodeling and heart function deterioration after myocardial infarction. *Circ Res* 2011;**108**:582-92.
89. Wang W, Wu L, Du X*, et al.* Anti-toll-like receptor 2 antibody inhibits nuclear factor kappa b activation and attenuates cardiac damage in high-fat-feeding rats. *Acta Biochim Biophys Sin (Shanghai)* 2019;**51**:347-55.
90. Zhai Y, Ao L, Yao Q*, et al.* Elevated expression of tlr2 in aging hearts exacerbates cardiac inflammatory response and adverse remodeling following ischemia and reperfusion injury. *Front Immunol* 2022;**13**:891570.
91. Li C, Yu Y, Li W*, et al.* Phycocyanin attenuates pulmonary fibrosis via the tlr2-myd88-nf-κb signaling pathway. *Sci Rep* 2017;**7**:5843.
92. Ji L, Xue R, Tang W*, et al.* Toll like receptor 2 knock-out attenuates carbon tetrachloride (ccl4)-induced liver fibrosis by downregulating mapk and nf-κb signaling pathways. *FEBS Lett* 2014;**588**:2095-100.
93. Shu M, Huang DD, Hung ZA, Hu XR, Zhang S. Inhibition of mapk and nf-κb signaling pathways alleviate carbon tetrachloride (ccl4)-induced liver fibrosis in toll-like receptor 5 (tlr5) deficiency mice. *Biochem Biophys Res Commun* 2016;**471**:233-9.
94. Zhao S, Dejanovic D, Yao P*, et al.* Selective deletion of myd88 signaling in α-sma positive cells ameliorates experimental intestinal fibrosis via post-transcriptional regulation. *Mucosal Immunol* 2020;**13**:665-78.
95. Wilson AS, Randall KL, Pettitt JA*, et al.* Neutrophil extracellular traps and their histones promote th17 cell differentiation directly via tlr2. *Nat Commun* 2022;**13**:528.
96. Satsangi J, Silverberg MS, Vermeire S, Colombel JF. The montreal classification of inflammatory bowel disease: Controversies, consensus, and implications. *Gut* 2006;**55**:749-53.
97. Rimola J, Planell N, Rodríguez S*, et al.* Characterization of inflammation and fibrosis in crohn's disease lesions by magnetic resonance imaging. *Am J Gastroenterol* 2015;**110**:432-40.
98. Chen W, Lu C, Hirota C*, et al.* Smooth muscle hyperplasia/hypertrophy is the most prominent histological change in crohn's fibrostenosing bowel strictures: A semiquantitative analysis by using a novel histological grading scheme. *J Crohns Colitis* 2017;**11**:92-104.
99. Gordon IO, Bettenworth D, Bokemeyer A*, et al.* International consensus to standardise histopathological scoring for small bowel strictures in crohn's disease. *Gut* 2021.

100. Gordon IO, Bettenworth D, Bokemeyer A*, et al.* Histopathology scoring systems of stenosis associated with small bowel crohn's disease: A systematic review. *Gastroenterology* 2020;**158**:137-50.e1.
101. Ceni E, Mello T, Polvani S*, et al.* The orphan nuclear receptor coup-tfii coordinates hypoxia-independent proangiogenic responses in hepatic stellate cells. *J Hepatol* 2017;**66**:754-64.
102. Carai P, Florit González L, Van Bruggen S*, et al.* Neutrophil inhibition improves acute inflammation in a murine model of viral myocarditis. *Cardiovasc Res* 2022.
103. Creyns B, Cremer J, Hoshino T*, et al.* Fibrogenesis in chronic dss colitis is not influenced by neutralisation of regulatory t cells, of major t helper cytokines or absence of il-13. *Sci Rep* 2019;**9**:10064.
104. Cooper HS, Murthy SN, Shah RS, Sedergran DJ. Clinicopathologic study of dextran sulfate sodium experimental murine colitis. *Lab Invest* 1993;**69**:238-49.
105. Love MI, Huber W, Anders S. Moderated estimation of fold change and dispersion for rna-seq data with deseq2. *Genome Biol* 2014;**15**:550.
106. Bindea G, Mlecnik B, Hackl H*, et al.* Cluego: A cytoscape plug-in to decipher functionally grouped gene ontology and pathway annotation networks. *Bioinformatics* 2009;**25**:1091-3.
107. Nijhuis A, Curciarello R, Mehta S*, et al.* Mcl-1 is modulated in crohn's disease fibrosis by mir-29b via il-6 and il-8. *Cell and Tissue Research* 2017;**368**:325-35.
108. Hofmann C, Chen N, Obermeier F*, et al.* C1q/tnf-related protein-3 (ctrp-3) is secreted by visceral adipose tissue and exerts antiinflammatory and antifibrotic effects in primary human colonic fibroblasts. *Inflamm Bowel Dis* 2011;**17**:2462-71.
109. Hutter S, van Haaften WT, Hünerwadel A*, et al.* Intestinal activation of ph-sensing receptor ogr1 [gpr68] contributes to fibrogenesis. *J Crohns Colitis* 2018;**12**:1348-58.
110. Biancheri P, Pender SL, Ammoscato F*, et al.* The role of interleukin 17 in crohn's disease-associated intestinal fibrosis. *Fibrogenesis Tissue Repair* 2013;**6**:13.
111. Leeb SN, Vogl D, Gunckel M*, et al.* Reduced migration of fibroblasts in inflammatory bowel disease: Role of inflammatory mediators and focal adhesion kinase. *Gastroenterology* 2003;**125**:1341-54.
112. Drury B, Hardisty G, Gray RD, Ho GT. Neutrophil extracellular traps in inflammatory bowel disease: Pathogenic mechanisms and clinical translation. *Cell Mol Gastroenterol Hepatol* 2021;**12**:321-33.
113. Gregory AD, Kliment CR, Metz HE*, et al.* Neutrophil elastase promotes myofibroblast differentiation in lung fibrosis. *J Leukoc Biol* 2015;**98**:143-52.
114. Lai HJ, Doan HT, Lin EY*, et al.* Histones of neutrophil extracellular traps directly disrupt the permeability and integrity of the intestinal epithelial barrier. *Inflamm Bowel Dis* 2023.
115. Maronek M, Gromova B, Liptak R*, et al.* Extracellular dna correlates with intestinal inflammation in chemically induced colitis in mice. *Cells* 2021;**10**.
116. Skendros P, Mitroulis I, Ritis K. Autophagy in neutrophils: From granulopoiesis to neutrophil extracellular traps. *Front Cell Dev Biol* 2018;**6**:109.

117. Papayannopoulos V, Metzler KD, Hakkim A, Zychlinsky A. Neutrophil elastase and myeloperoxidase regulate the formation of neutrophil extracellular traps. *J Cell Biol* 2010;**191**:677-91.